ESTIMATING FLOW AND TRANSPORT

PARAMETERS OF UNSATURATED

POROUS MEDIA

By

JOHN SPARKMAN TYNER

Bachelor of Science
University of Oklahoma
Norman, Oklahoma
1990

Master of Science
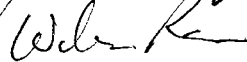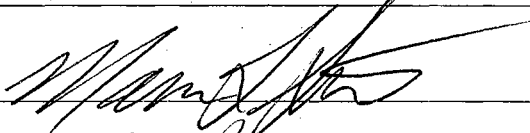San Diego State University
San Diego, California
1998

Submitted to the Faculty of the
Graduate College of the
Oklahoma State University
in partial fulfillment of
the requirement for
the Degree of
DOCTOR OF PHILOSOPHY
August, 2001

ESTIMATING FLOW AND TRANSPORT

PARAMETERS OF UNSATURATED

POROUS MEDIA

Thesis Approved:

_____
Thesis Advisor

_____

_____

_____

_____
Dean of the Graduate College

ACKNOWLEDGEMENTS

I wish to express the utmost appreciation to my advisor and friend, Dr. Glenn Brown, for his encouragement, support, and candid advice throughout my studies. I could not have wished for a more outstanding advisor. I would also like to extend gratitude to my other committee members, Dr. Marvin L. Stone, Dr. Ronald Elliott, and Dr. William R. Raun for their valuable assistance. Financial support received from the Sitlington Enriched Scholarship and the Soil Fertility Research and Educational Advisory Board allowed my efforts to stay focused on my doctoral studies. The research portion of the Sitlington Enriched Scholarship enabled my attendance at professional conferences, which was a pertinent portion of my education.

My darling wife Jane has been loving and patient throughout my studies and has sacrificed much en route to this destination. She was often my inspiration to push forward when difficulties arose. Knowledge of Mom and Dad, and my siblings' love was also very empowering and has allowed me to overcome many challenging obstacles throughout my life. Lastly, I must thanks Gramps and Granny for making me believe I was such a special young boy during my summers in Caddo. I will forever cherish those hot summer days feeding chickens and snapping beans. When Gramps goes to town and brags on you at the Dairy Queen, good things can happen.

TABLE OF CONTENTS

LIST OF TABLES

LIST OF FIGURES

CHAPTER I

BACKGROUND, REVIEW, AND OBJECTIVES

1.1 Problem Statement

The description of fluid and solute transport within unsaturated porous media is necessary for a multitude of issues that engineers and scientist must address. Because the vadose zone is not an exploitable source of fresh water, it has been overlooked historically, and knowledge of unsaturated transport was slow to develop. However, as interest in agriculture, water resources, and environmental issues has grown, the vadose zone has received increased consideration. Compared to saturated conditions, the vadose zone is more complex due to the fact that flow is often strongly related to water content and water content history. Due to this added complexity, the vadose zone is often poorly described.

Equations describing unsaturated flow are available, but measurement of the parameters needed to solve the flow equations is a difficult task. It often takes weeks or even months to measure soil hydraulic properties. Estimating these functions from easily measurable parameters is also difficult because the functions may vary by orders of magnitude between seemingly similar soil samples.

The purpose of this study is to provide additional methods to measure and describe unsaturated transport. More specifically, the objectives are:

- to develop an improved method of unsaturated hydraulic function measurement,

- to extend the use of the Chloride Mass Balance Method to non-arid, agricultural areas, and,

- to provide a historical interpretation of recharge, evapotranspiration, and runoff at a KCl fertilized field using deep continuous soil chloride profiles in conjunction with long-term meteorological data.

As detailed in the Research Focus to follow, these three objectives will be addressed in Chapters II, III, and IV, respectively. Each of these objectives resulted from attempts to estimate vertical downward nitrate flux beneath winter wheat plots at the Stillwater Agricultural Experiment Station.

The initial attempt at nitrate flux measurement was to determine the water recharge by estimating soil hydraulic functions from water retention measurements. Hydraulic parameters describing these functions would be used within a numerical unsaturated groundwater model to estimate recharge. The estimated recharge along with measured nitrate concentrations in the soil column would then allow for calculation of the nitrate flux. Unfortunately, measurement of the water retention function is a very difficult and time consuming procedure. Furthermore extrapolation of the hydraulic conductivity function from such measurements adds an additional abstraction leading to less confidence in the resultant nitrate flux estimates. These difficulties led directly to the first two objectives of this dissertation: a better means to measure hydraulic functions, and application of the Chloride Mass Balance Method in a non-arid agricultural setting. The third objective resulted from the desire to interpret water solute flux beneath the

winter wheat plots without the assumption of steady state conditions, thus allowing for interpretation of the historical recharge record.

1.2 Describing Unsaturated Porous Media Transport

In 1856, Henri Darcy was the first to assert that the volumetric flow rate of water through a porous medium (Q) is proportional to its wetted cross sectional area (A), multiplied by a proportionality constant (hydraulic conductivity) (K), multiplied by the difference in head (Δh), divided by the distance over which the head was measured (ΔL) [*Darcy*, 1856].

$$Q = -KA\left(\frac{\Delta h}{\Delta L}\right) \tag{1.1}$$

This conclusion was proclaimed after confirming its existence using a saturated flow test. This simple relationship is also valid for unsaturated flow [*Buckingham*, 1907], although the hydraulic conductivity and head become strong functions of water content that vary over many orders of magnitude.

The measurement of saturated hydraulic conductivity and head is easily conducted and the two are generally considered to be single-valued functions, since by definition the water content is constant. In the vadose zone, hydraulic conductivity and head must be measured over a range of water contents. Since the hydraulic conductivity becomes very small at low water contents, most methods to measure these functions require long periods of time to reach equilibrium at each water content measured.

Other means to determine hydraulic parameters include the use of tracers. Artificial and naturally available tracers often enable the path and flow rate of water and solutes to be determined. Solving groundwater flow equations in an inverse manner

3

using input derived from tracer experiments may allow for computation of the hydraulic parameters. Such inverse methods are frequently poorly constrained having multiple possible hydraulic functions.

1.3 Research Focus

Chapter II, which has been submitted for publication, describes a rapid method to describe unsaturated hydraulic functions. The technique consists of the imbibition of water into a soil column followed by a quasi-analytic solution of the water content profile that enables determination of hydraulic parameters. These parameters are commonly used in numerical groundwater models to describe the pertinent hydraulic functions including the hydraulic conductivity and water retention functions.

The method compares favorably to direct measurements of hydraulic functions due to the time and expense of direct measurements. It is also an improvement to estimates of the unsaturated hydraulic conductivity function based on measurements of water retention because such estimates are derived from static measurements of head versus water content, not an actual unsaturated flow event.

Chapter III describes the application of the Chloride Mass Balance Method to estimate recharge in a sub-humid agricultural environment. Typically the use of chloride mass balance is constrained to arid regions due to the requirement of extensive concentration of chloride in the soil column. The long-term application of KCl to the study area provided sufficient chloride to carry out the method in a much wetter environment than is normally considered feasible.

Chapter IV uses a Chloride Mass Balance Approach in conjunction with historical meteorological data to estimate temporal variations of recharge. Using the mean

recharge calculated in Chapter III along with measured precipitation, and estimates of evapotranspiration and runoff, the sum of evapotranspiration and runoff is properly scaled using a simple water balance equation. Such an approach allows insight into recharge versus weather over time, which might be useful for agricultural planning.

1.4 Future Recommendations

The objectives of this research were to provide for additional means to estimate transport of water and solutes in unsaturated porous media. These objectives led to a new method to describe hydraulic functions, an extension of the applicability of the Chloride Mass Balance Method, and a means to refine Chloride Mass Balance recharge estimates over time using historical meteorological information. These objectives have been accomplished.

Future research regarding Chapter II includes three areas. First, further application of the method is needed to ensure its applicability to different soil types and moisture contents. This is necessary to ensure reliability and to help publicize the method. Given the difficulty and cost of present methods to measure hydraulic properties, a market for the method seems to be available.

Second, the mathematical derivation of hydraulic parameters using the new method is difficult and lengthy. A computer program that allows input of raw data and calculates hydraulic parameters would enable a much larger audience to take advantage of this method. Without such a computer program, its potential usage is likely limited to researchers. As previously stated, the method has potential to become widely used, but a user-friendly computer program must be provided for this to occur.

Third, the method could potentially be extended to include two viscous, non-compressible phase flow such as a water/oil system. *McWorter and Sunada* [1990] describe an exact mathematical solution for such a system, which is similar to the solution used in Chapter II. The inclusion of two viscous, non-compressible phase flow might lead to application within the petroleum and environmental industries.

Future research of Chapter III includes applying the method at additional sites to help ensure that water fluxes calculated for winter wheat production at the Stillwater Agricultural Experiment Station are representative for winter wheat production in other nearby winter wheat producing locations. The confidence of conclusions from Chapter IV would be increased if additional weather parameters were available to increase the reliability of the non-scaled evapotranspiration estimate. Varying the input of root density and curve number over time to better represent the winter wheat growth cycle might enable better fitting of chloride concentration distributions. Additionally more measured weather parameters would allow for the comparison of evapotranspiration as estimated by numerous methods.

1.5 References

Buckingham, E., Studies on the movement of soil moisture. *Bureau of Soils Bulletin 38,* Washington D.C., U.S. Dept. of Ag., 1907.

Darcy, H.. *Les Fontaines Publiques de la Ville de Dijon.* Dalmont, Paris. 647 p. & atlas.,1856.

McWhorter, D. B., D. K. Sunada, Exact integral solutions for two-phase flow. *Wat. Res. Res.,* 26:399-413., 1956.

CHAPTER II

A RAPID METHOD TO MEASURE UNSATURATED SOIL PROPERTIES

2.1 Abstract

Current methods to determine unsaturated soil properties are expensive, difficult, and time consuming. A new procedure is presented that quickly estimates the unsaturated hydraulic conductivity, diffusivity, water retention, and sorptivity functions by way of a Bruce-Klute test. The method is much easier than direct measurement of unsaturated soil functions since a Bruce-Klute test can be conducted with little overhead in less than an hour. It also compares favorably to estimating soil properties from a water retention curve since a Bruce-Klute test is dynamic, thereby removing the abstraction from static measurements to fluid resistance. The method is applied to a silt loam soil and results are compared to hydraulic properties defined from a water retention curve. Strengths and weaknesses of the method are discussed and the sensitivity to various parameters is presented.

2.2 Introduction

Knowledge of soil hydraulic properties is required to estimate fluid flow in unsaturated porous media. Commonly, numerical models are employed to estimate fluid flow in a variety of settings. Although much effort has been expended to increase the sophistication of numerical models, lack of sufficient model input is arguably a larger

problem for many modelers. Modelers require hydraulic parameters from an increasing number of soil samples to more fully describe a setting. Because direct measurement of unsaturated hydraulic functions is difficult and expensive, properties are often estimated by applying the *Muelem* [1976] or *Burdine* [1953] model to a water retention curve described by *Brooks and Corey* [1966] or *van Genuchten* [1980]. Although this procedure limits the number of laboratory measurements required to describe soil parameters, it introduces the possibility for error due to an additional theoretical abstraction. Furthermore, measurement of water retention is also a costly, difficult, and tedious process. Thus, many practitioners have adopted the additional abstraction of estimating soil water retention from grain size distribution, bulk density, and other easily measured soil properties [*Arya and Paris*, 1981]. More recent attempts to measure unsaturated hydraulic properties include use of ultra high-speed centrifuge technology [*Conca and Wright*, 1998]. The cost of this technology has limited its usage and the method is not without its theoretical critics.

Instead of fitting soil parameters to a water retention curve, we propose fitting them to the data resulting from a Bruce-Klute test. The Bruce-Klute test records volumetric moisture content *(θ)* at different distances from a constant head inlet *(x)* over time *(t)*. The resulting data set, *λ(θ)* where $\lambda = x/\sqrt{t}$, is plotted. The wetting profile, *λ(θ)*, is also generated from a purely theoretical method using van Genuchten's description of diffusivity, in conjunction with *Philip and Knight's* [1974] fractional flow solution to a Bruce-Klute boundary condition. By fitting the generated wetting profile to the measured data, values for the van Genuchten soil hydraulic parameters can be optimized. The optimized van Genuchten soil hydraulic parameters allow for estimation

of the water retention, diffusivity, and sorptivity at any given initial and inlet water content functions. An independently measured value for saturated hydraulic conductivity allows for the estimation of the unsaturated hydraulic conductivity function.

This method has three major advantages to estimating hydraulic parameters via water retention measurements. First, a Bruce-Klute test can be conducted in less than an hour and requires much less finesse than water retention measurements. Second, the Bruce-Klute test is a wetting procedure instead of the draining procedure usually used to obtain water retention measurements. Since many hydraulic properties are hysteretic and we are most often interested in wetting conditions, hydraulic properties derived from a wetting procedure may be preferable. Third, hydraulic parameters are estimated by predicting the results of a Bruce-Klute test, which ensures the parameters can model water flow for at least one setting. This is in contrast to estimating parameters from $\psi(\theta)$ where no confirmation of the validity of parameters to predict flow is available.

2.3 Theory

2.31 van Genuchten Parameters

This method uses *van Genuchten's* [1980] expression for water retention, although similar versions utilizing *Brooks and Corey* [1966] or numerous other versions could be used. van Genuchten describes the water retention curve by

$$\Theta = \frac{\theta - \theta_r}{\theta_s - \theta_r} = \left[\frac{1}{1 + (\alpha\psi)^n} \right]^m , \qquad (2\text{-}1)$$

where Θ is the normalized water content; α, m, n, θ_s, and θ_r are fitting parameters; and ψ is the soil suction. θ_s and θ_r represent the saturated water content and residual water content respectively. By letting

$$m = 1 - 1/n \qquad 0 < m < 1 \qquad (2\text{-}2)$$

and applying *Muelem* [1976], van Genuchten uses his expression for water retention to derive an expression for unsaturated hydraulic conductivity,

$$K(\Theta) = K_s \Theta^{1/2} \left[1 - \left(1 - \Theta^{1/m} \right)^m \right]^2, \qquad (2\text{-}3)$$

where K_s is the saturated hydraulic conductivity. Using the definition of diffusivity [*Klute*, 1952],

$$D(\theta) = K(\theta) \frac{dh}{d\theta}, \qquad (2\text{-}4)$$

van Genuchten also provides an expression for $D(\Theta)$ in terms of his soil parameters,

$$D(\Theta) = \left(\frac{K_s}{\alpha} \right) \frac{1-m}{m(\theta_s - \theta_r)} \Theta^{(1/2 - 1/m)} \left[\left(1 - \Theta^{1/m} \right)^{-m} + \left(1 - \Theta^{1/m} \right)^m - 2 \right]. \qquad (2\text{-}5)$$

Summarizing, van Genuchten's expressions for unsaturated hydraulic functions contains six parameters, α, m, n, θ_s, θ_r, and K_s. As is common practice, we apply (2-2) to reduce the number of required parameters to five.

2.32 Bruce-Klute Test

Bruce and Klute [1956] provide a convenient method to measure $D(\theta)$. The method represents horizontal, semi-infinite, one-dimensional flow as

$$\frac{\partial \theta}{\partial t} = \frac{\partial}{\partial x} \left(D(\theta) \frac{\partial \theta}{\partial x} \right), \qquad (2\text{-}6)$$

where x is the horizontal distance from the inlet, and t is the elapsed time. The initial and boundary conditions for the test are

$$\theta = \theta_n \qquad \text{for } x > 0 \quad \text{and} \quad t = 0,$$

$$\theta = \theta_o \qquad \text{for } x = 0 \quad \text{and} \quad t > 0, \tag{2-7}$$

$$\theta = \theta_n \qquad \text{for } x = \infty \text{ and } t > 0,$$

where θ_n is the antecedent water content and θ_o is the inlet water content. These conditions are traditionally referred to as the constant concentration condition. The *Boltzman* [1894] transform reduces (2-6) and (2-7) to the ordinary differential equation,

$$-\frac{\lambda}{2}\frac{d\theta}{d\lambda} = \frac{d}{d\lambda}\left(D(\theta)\frac{d\theta}{d\lambda}\right), \tag{2-8}$$

subject to,

$$\theta = \theta_n \qquad \text{for } \lambda = \infty$$

$$\tag{2-9}$$

$$\theta = \theta_o \qquad \text{for } \lambda = 0$$

where $\lambda = x/\sqrt{t}$. Integration of (2-8) with respect to λ yields

$$D(\theta) = -\frac{1}{2}\left(\frac{d\lambda}{d\theta}\right)\int_{\theta_n}^{\theta}\lambda\, d\theta, \tag{2-10}$$

which is represented graphically in Figure 2-1. *Philip* [1969] showed that the inlet flux, q_o, is given by

$$q_o = \frac{1}{2}S(\theta_n,\theta_0)t^{-\frac{1}{2}} \tag{2-11}$$

where q_o is the water flux at the inlet $(x = 0)$ and $S(\theta_n, \theta_o)$ is the sorptivity. $S(\theta_n, \theta_o)$ is defined as

$$S(\theta_n,\theta_0) = \int_{\theta_n}^{\theta_o}\lambda\, d\theta. \tag{2-12}$$

11

and is a constant for given values of θ_n and θ_o.

Equation (2-10) provides a direct method to calculate $D(\theta)$, however its application is problematic for three reasons.

I. The slope of $\lambda(\theta)$ near the inlet and wetting front are difficult to measure accurately due to the very small and large slopes respectively.

II. The calculated diffusivities are tabular, which make their application within numerical models complicated.

III. The calculated $D(\theta)$ values are not necessarily consistent with the measured $\lambda(\theta)$ data from the Bruce-Klute test. That is, there is no measure of the ability for $D(\theta)$ to accurately predict the measured $\lambda(\theta)$.

Several papers have suggested methods to address difficulties (I and II) by initially fitting a function to the measured $\lambda(\theta)$ data and then numerically determining the slope and area of the curve [*McBride and Horton*, 1985; *Meyer and Warrick*, 1990]. A weakness common to these methods is that they do not address difficulty (III). Essentially, they do not ensure that the estimated $D(\theta)$ values will predict the measured $\lambda(\theta)$ curve under the conditions provided during the data collection for such a curve. Given that $D(\theta)$ at high water contents is large and sensitive to the difficult interpretation of $d\lambda/d\theta$, small errors in the interpretation of $d\lambda/d\theta$ can lead to large errors of $D(\theta)$ near saturation. Of course these errors are not apparent until the estimated $D(\theta)$ values have been used to predict the measured $\lambda(\theta)$ curve.

While developing equations to describe two-phase constant concentration boundaries, *McWhorter* (1971) introduced the fractional flow, *F(θ)*, where

$$F(\theta) = \frac{q(\theta)}{q_0} \qquad (2\text{-}13)$$

q(θ) is the flux density, and q_0 is the flux density at $x = 0$. Inspection of (2-13) reveals that *F(θ)* encompasses values from one at $\theta = \theta_0$ to zero at $\theta = \theta_n$. Using the same definition for *F(θ)*, *Philip* [1973] derived a similar expression for fractional flow given as

$$F(\theta) = \frac{\int_{\theta_n}^{\theta} \lambda(\theta) d\theta}{\int_{\theta_n}^{\theta_0} \lambda(\theta) d\theta} \qquad (2\text{-}14)$$

Philip and Knight [1974] provide expressions for *S(θ_n, θ_o)* and *λ(θ)* as

$$S = \left[2 \int_{\theta_n}^{\theta_0} \frac{(\theta - \theta_0) D(\theta)}{F(\theta)} d\theta \right]^{1/2} \qquad (2\text{-}15)$$

$$\lambda(\theta) = \frac{2}{S} \int_{\theta}^{\theta_0} \frac{D(\theta)}{F(\theta)} d\theta \qquad (2\text{-}16)$$

and an exact, quasi-analytical solution of (2-14) using the iterative procedure

$$F(\theta)_{i+1} = \frac{\int_{\theta_n}^{\theta} \left(\int_{\theta}^{\theta_0} \frac{D(\theta)}{F(\theta)_i} d\theta \right) d\theta}{\int_{\theta_n}^{\theta_0} \frac{(\theta - \theta_n) D(\theta)}{F(\theta)_i} d\theta} = 1 - \frac{\int_{\theta}^{\theta_0} \frac{(\beta - \theta) D(\beta)}{F_i(\beta)} d\beta}{\int_{\theta_n}^{\theta_0} \frac{(\theta - \theta_n) D(\theta)}{F(\theta)_i} d\theta} \qquad (2\text{-}17)$$

where *i* represents the iteration of *F(θ)*, and *β* is a variable of integration. Equation (2-17) is a special case of *McWhorter's* [1971] solution for horizontal flow of two viscous

fluids. The rightmost expression is used during computations of $F(\theta)$. As $F(\theta)_i \rightarrow F(\theta)_{i+1}$, (2-17) converges to the exact solution

$$F(\theta) = \frac{\int_{\theta_n}^{\theta} \left(\int_{\theta}^{\theta_0} \frac{D(\theta)}{F(\theta)} d\theta \right) d\theta}{\int_{\theta_n}^{\theta_0} \frac{(\theta - \theta_n)D(\theta)}{F(\theta)} d\theta} \qquad (2-18)$$

rapidly for all $D(\theta)$ represented by a monotonically increasing function including $D(\theta)$ defined using van Genuchten soil parameters. *Brown and McWhorter* [1990] found that the first guess,

$$F(\theta)_1 = \frac{(\theta - \theta_n)}{(\theta_o - \theta_n)} \qquad (2-19)$$

provides a stable convergence to a final estimate even for non-monotonic diffusivity functions. A useful expression may be obtained by the substitution of (2-12) into (2-14) followed by differentiation with respect to θ which yields [*Brown*, 1987]

$$\lambda(\theta) = S(\theta_n, \theta_0) \frac{dF}{d\theta} \qquad (2-20)$$

Equation (2-20) provides a convenient and accurate expression for numerical solutions.

2.34 Clothier et al's and Warrick's Procedures

Clothier et al. [1983] showed the difficulty of evaluation of (2-10) and then provided a method to ensure the estimated $D(\theta)$ is consistent with measured $\lambda(\theta)$. They first fit a free-hand curve through measured $\lambda(\theta)$ data, and using (2-10), calculated $D(\theta)$. Next, $F(\theta)$ and $S(\theta_n, \theta_o)$ were determined using (2-14) and (2-15), respectively. Finally $\lambda(\theta)$ was estimated using (2-16) and compared to the measured $\lambda(\theta)$. The estimate for

$S(\theta_n, \theta_o)$ using (2-15) was found to be 11% larger than $S(\theta_n, \theta_o)$ calculated from (2-12) using the measured data. They emphasized that this disparity, "may be fortuitously small." To avoid the discrepancy between measured and predicted $\lambda(\theta)$, they proposed estimating $D(\theta)$ using analytical expressions derived in *Philip* [1960] that allow expressions for $D(\theta)$ to be fit directly to the measured $\lambda(\theta)$, thereby ensuring proper scaling of measured and predicted $S(\theta_n, \theta_o)$. A drawback of this method is that it does not utilize familiar soil parameters such as *Brooks and Corey* [1966] or *van Genuchten* [1980], thereby limiting the utilization of such parameters beyond expressions for $D(\theta)$.

McBride and Horton [1985] state that their method to determine $D(\theta)$ from a Bruce-Klute test compares favorably to that of *Clothier et al.* [1983]. This statement is founded on the fact that their $\lambda(\theta)$ function fits measured $\lambda(\theta)$ data better than that of Clothier et al. They have failed to show that $D(\theta)$ calculated by their method will accurately predict the measured $\lambda(\theta)$ as is done analytically in the Clothier et al. solution. There exists a multitude of $\lambda(\theta)$ expressions that could be used to simply fit measured $\lambda(\theta)$ data. Since the ultimate goal of measuring hydraulic properties is to predict flow, arguments that one $\lambda(\theta)$ expression fits measured $\lambda(\theta)$ data slightly better than another are trivial unless they can also be shown to better predict $\lambda(\theta)$ from the estimates of $D(\theta)$.

Using several common $D(\theta)$ functions including (2-5), *Warrick* [1994] optimized soil parameters using the *Philip* [1969] finite difference solution of the constant concentration condition. This solution is similar to that of *Philip and Knight* [1974] in that it allows $D(\theta)$ to predict $\lambda(\theta)$. By assuming θ_s and θ_r were known and equal to θ_0

and θ_n, respectively, the predicted $\lambda(\theta)$ was fit to the measured $\lambda(\theta)$ by simultaneously optimizing the van Genuchten m and a lumped parameter $A(m)$

$$A(m) = \left[\frac{K_s}{\alpha(\theta_s - \theta_r)} \right]^{0.5} \tag{2-21}$$

Since $D(\Theta)$ in (2-5) approaches infinity as θ_0 approaches θ_s, it is assumed some type of numerical procedure was used to approximate $D(\theta)$ at saturation, possibly the estimation method presented in *Warrick, et al.* [1985]. Essentially Warrick's method starts with five unknown parameters (K_s, α, m, θ_s, and θ_r), assumes two are known (θ_s, and θ_r) and optimizes two others (m and $A(m)$). Selection of a $D(\theta)$ function whose parameters are related to the water retention curve and unsaturated hydraulic conductivity function is quite appealing. Given independent knowledge of θ_s, θ_r and either K_s or α, a soil's hydraulic functions can be fully described. However, measurement of K_s, α, θ_s, and θ_r requires laboratory procedures that are difficult, expensive and time consuming using traditional techniques.

2.4 New Method

Like *Warrick* [1994], we choose to fit van Genuchten's description of $D(\theta)$, (2-5), to the measured $\lambda(\theta)$. We prefer to solve the constant concentration condition using *Philip and Knight* [1974] due to both its relative ease and more analytical basis compared to *Philip* [1969]. Additionally, our method offers two distinct improvements over previous methods. First, m is determined independently of K_s/α instead of using a lumped parameter such as (2-21). Second, we provide a method to estimate θ_r from a single measurement of ψ versus θ, which is important since θ_r will not normally be

16

known. Applying the Boltzman transform to the collected data results in the calculation of $\lambda(\theta)$. The λ axis is normalized to

$$\Lambda(\theta) = \lambda(\theta)/\lambda_{wf} \qquad (2\text{-}22)$$

where λ_{wf} is the largest value of λ such that $\theta > \theta_n$ (Figure 2-2).

An estimate of $D(\Theta)$ is calculated using (2-5) with an initial guess for n, unity for the ratio K_s/α, θ_s is set equal to the porosity, and θ_r is initially estimated based on soil type or prior knowledge. Next, the initial $D(\Theta)$ and $F(\theta)_l$ are entered into (2-17) followed by iteration until convergence of $F(\theta)$ is achieved. *Philip and Knight* [1974] and personal experience demonstrate that four iterations are adequate for most soils. A theoretical water profile, $\lambda(\theta)$, is predicted using (2-15) and (2-20), and is then normalized to $\Lambda(\theta)$ using (2-21). By normalizing $\lambda(\theta)$ to $\Lambda(\theta)$, the influence of the lumped parameter K_s/α is removed, which allows for optimization of n independent of K_s/α (Figure 2-3). Next, we optimize the value of n by minimizing the weighted absolute value of differences between measured and predicted $\Lambda(\theta)$.

The functional independence of $\Lambda(\theta)$ and K_s/α can be demonstrated by noting from (2-2) and (2-5) that the predicted $D(\theta)$ is linearly related to K_s/α and is a complex function of n. Substituting (2-5) into (2-18) reveals that $F(\theta)$ is independent of K_s/α since it resides once in the numerator and denominator. However, n cannot be reduced from (2-18) revealing that $F(\theta)$ and n are dependent. Equation (2-15) shows that $S(\theta_n, \theta_o)$ is a function of K_s/α and n since $D(\theta)$ is only present in the numerator. Thus, when (2-

20) is substituted into the numerator and denominator of the right side of (2-21), $S(\theta_n, \theta_o)$ is cancelled and $\Lambda(\theta)$ is shown to be a function of n, but not K_s/α.

Using the previously determined n, we compare the predicted $\lambda(\theta)$ with the measured $\lambda(\theta)$ to optimize K_s/α, again using the weighted absolute value of differences (Figure 2-4). We can also check to verify that $S(\theta_n, \theta_o)$, given by (2-12), is equal to the $S(\theta_n, \theta_o)$ delivered to the column. Agreement of the experimental and theoretical $S(\theta_n, \theta_o)$ provides evidence that measurement of $\lambda(\theta)$ was conducted accurately.

The only parameter yet to be determined is θ_r. The values for α, m, and n are all functions of the initial estimate of θ_r. Since θ_r is a fitting parameter and is only defined in terms of fitting (2-1) to measured $\psi(\theta)$ data, it cannot be measured directly. θ_r is determined by first collecting a single measurement of ψ versus θ at a moderately dry water content. Next, we select a new estimate for θ_r that allows the prediction of $\psi(\theta)$ by letting (2-1) pass through the measurement of ψ versus θ. Using the second estimate for θ_r, α and n are re-optimized using Philip and Knight [1974] followed by another optimization of θ_r. This iterative process is repeated until subsequent estimates of θ_r converge.

Restating the procedure:

1. Start with six unknown hydraulic parameters (α, m, n, θ_s, θ_r, and K_s) and apply (2-2) to determine m in terms of n.

2. Measure or estimate θ_s based on the porosity.

3. Conduct Bruce-Klute test and normalize the data by (2-21).

4. Temporarily assume a value for θ_r based on soil type or other measure.

5. Use *Philip and Knight's* [1974] solution to obtain a best-fit estimate of n.

6. Using the non-normalized $\lambda(\theta)$ data and the previously determined n, conduct an additional solution of Philip and Knight's [1974] solution to obtain a best fit estimate of K_s/α.

7. Independently measure K_s and calculate α.

8. Measure a single point on the $\psi(\theta)$ curve. Using the estimates for α and n, estimate θ_r by applying (2-1).

9. Using the new value for θ_r, iterate through steps 5 to 8, with the exception of the measurement of K_s and $\psi(\theta)$, until convergence of θ_r is achieved.

2.5 Laboratory Procedures

Soil is uniformly packed with a uniform water content, θ_n, into a 100 to 200 mm long, 35 mm diameter clear acrylic column. A clear column allows for visual verification of the water front location during testing, but is not necessary. Larger diameter columns are allowable for fine textured soils, however coarse textured soils may exhibit non-vertical wetting fronts due to gravitational effects. Field samples may be used if they are homogenous and if water content is allowed to equilibrate before testing.

Water is injected into the soil column with a programmable syringe pump at a rate following (2-11) [*Brown and Allred*, 1992]. Use of a syringe pump, instead of a traditional Mariotte flask, allows the inlet boundary condition to be maintained at any desired water content. In particular, if it is desired to maintain a relatively small θ_0 while testing a fine-grained soil, the large negative pressure required makes a Mariotte flask impractical. Use of Mariottes also tends to cause $d\lambda/d\theta$ to become concave upward near

19

the inlet. *Bruce and Klute* [1956] discuss this behavior and the fact that it leads to calculation of a maximum $D(\theta)$ at less than saturation. *Brown and Allred* [1992] conducted a direct comparison of the two types of inlets and their results show that a concave upward $d\lambda/d\theta$ is only present with the Mariotte flask induced boundary condition. Equation (2-5) predicts that $D(\Theta) \to \infty$ as $\Theta \to 1$ which is consistent with a concave downward $d\lambda/d\theta$ near the inlet as produced by the syringe pump induced boundary condition.

During imbibition the volumetric water content is measured at various distances from the inlet over time using gamma ray attention procedures [*Gardner*, 1986]. Although the required $\lambda(\theta)$ curve can be measured from a single location, measurement from multiple locations over time allows confirmation that infiltration is following Boltzman normalization theory by verifying that all of the $\lambda(\theta)$ data lay atop a single curve. Alternatively, one can dissect the column immediately after imbibition and measure the water content gravimetrically a described in *Bruce and Klute* [1956]. Measurement of θ at a single time or location does not enable confirmation of Boltzman normalization theory and fewer useful data can be collected. Additionally, measuring θ gravimetrically hinders the use of field-collected samples since the columns must be quickly dissected following imbibition. Quick dissection of unconsolidated material would be difficult given the types of column sheathes often used. Consolidated material might also be difficult to dissect quickly due to the hardness of the sample itself. Data collection must cease prior to the water front advancing to the end of the column to meet the semi-infinite boundary condition of (2-9).

2.6 Results

This method was applied to the Slaughterville sandy loam (Thermic Udic Haplustoll), which was collected near Perkins, Oklahoma. The hand packed soil had a dry bulk density of 1480 Kgm^{-3} and a porosity of 0.44 estimated from an assumed particle density of 2650 Kgm^{-3}. A $S(\theta_n, \theta_o)$ of 8.9 E-6 m^{2}s$^{-1/2}$ was used to program the syringe pump flux. Water content, θ, was measured at 100 and 110 mm from the inlet; the resulting $\lambda(\theta)$ plot is shown in Figure 2-2. Saturated water content, θ_s, was assumed to equal the porosity, and θ_r was initially estimated as 0.065 based on soil type [*Carsel and Parish*, 1988]. Initial and inlet water contents, θ_n and θ_0, were set to measured values of 0.035 and 0.37 respectively. After normalizing $\lambda(\theta)$ to $\Lambda(\theta)$, the solution was used to optimize $n = 1.89$ (Figure 2-3). Using this estimate for n, the $\lambda(\theta)$ curve was used in conjunction with the Philip and Knight [1974] solution to optimize $K_s/\alpha = 2.24$ E-5 m^{2}s^{-1} as shown in Figure 2-4. Saturated hydraulic conductivity, K_s, was measured independently by means of a constant head permeameter and found to be 6.4 E-5 ms^{-1}, which leads to an α of 2.86 m^{-1}.

A single measurement of $\psi = 153$ m versus $\theta = 0.058$ was collected using pressure plates. Optimizing (2-1) for θ_r achieves $\theta_r = 0.056$. The solutions converged after three additional iterations. Table 2-1 presents the method's estimates of n, α, and θ_r for each iteration. Similar results were achieved using an initial $\theta_r = 0.00$. Estimates for n, α, and θ_r were also predicted using the RETC code [*van Genuchten et al.*, 1991] to curve fit an independently measured $\psi(\theta)$ distribution and are shown in Figure 2-5.

Table 2-1. Iteration of Method and Parameters Derived from $\psi(\theta)$ and RETC

Iteration Number	θ_r (input)	N	α [m^{-1}]	θ_r (output)
1	.065	1.89	2.86	.056
2	.056	1.78	2.56	.055
3	.055	1.77	2.50	.054
4	.054	1.76	2.49	.054
1	.000	1.42	1.41	.013
3	.029	1.55	1.76	.040
7	.053	1.75	2.48	.054
8	.054	1.76	2.49	.054
$\psi(\theta)$ and RETC	N/A	4.62	1.91	.064

Figure 2-6 presents the measured $\lambda(\theta)$, $\lambda(\theta)$ predicted by this method, and $\lambda(\theta)$ predicted from $\psi(\theta)$ derived parameters in conjunction with the Philip and Knight [1974] solution. It is obvious that this method has performed much better predicting the flow than using hydraulic parameters defined from $\psi(\theta)$. Of course this is to be expected since the method was optimized to $\lambda(\theta)$. Using the estimated hydraulic parameters from the final iteration: $\psi(\theta)$, $K(\theta)$, and $D(\theta)$ are easily calculated using (2-1), (2-3), and (2-5).

The sorptivity, $S(\theta_n, \theta_o)$ can be estimated for any chosen value of θ_n and θ_o using the Philip and Knight [1974] solution in conjunction with the previously determined hydraulic parameters as shown in Figure 2-7. The figure shows lines of equal sorptivity as a function of inlet and initial water contents. As can be seen, $S(\theta_n, \theta_o)$ varies from zero to infinity with a four order of magnitude variation in the region of common interest. The infinite $S(\theta_n, \theta_o)$ predicted is a result of the infinite $D(\Theta)$ predicted by (2-5) as θ_o approaches θ_s. Of course, an infinite $S(\theta_n, \theta_o)$ is physically infeasible. The results imply that this type of test is best performed at inlet water contents slightly less than saturated.

2.7 Conclusions

This paper provides a significant advance toward effectively describing hydraulic parameters from a simple infiltration experiment. Using a Bruce-Klute test to measure a specific wetting profile, van Genuchten-Muelem's description of $D(\theta)$ is optimized using Philip and Knight's [1974] constant concentration solution to predict the previously measured wetting profile. The van Genuchten soil parameters defining $D(\theta)$ in conjunction with an independently measured K_s allow for the estimation of $K(\theta)$, $\psi(\theta)$, and $S(\theta_n, \theta_o)$. A procedure is also provided to increase the accuracy of the predicted hydraulic parameters using a single measurement of ψ versus θ which enables the optimization of θ_r.

This method compares favorably to the determination of hydraulic parameters from water retention measurements in two ways. First, conducting a Bruce-Klute test usually takes less than an hour, whereas measurement of the water retention function can take days or weeks. The Bruce-Klute data presented in this paper were collected in 55

minutes. Second, this method optimizes the hydraulic parameters to a measured flow event instead of relying on static water retention measurements. Given the demand for more accurate and economical procedures to determine unsaturated soil parameters, this type of approach appears to have potential for more widespread application in the future.

2.8 Acknowledgement

2.9 References

Arya, L. M., and J. F. Paris, A physicoempirical model to predict the soil moisture characteristics from particle-size distribution and bulk density data. *Soil Sci. Soc. Am. J.*, 45:1023-1030, 1981.

Boltzman, L., Zur Integraten der diffusions gleichung bei variabeln diffusions coefficienten. *Ann. Physics.*, 53:959-964, 1894.

Brooks, R. H. and A. T. Corey, Properties of porous media affecting fluid flow. *ASAE J. Irr. Drainage Div.*, IR2:61-87, 1966.

Brown, G. O., *Solute Transport by a Volatile Solvent*. Ph.D. Dissertation, Department of Civil Engineering, Colorado State University, Fort Collins, CO., 1987.

Brown, G. O. and B. Allred, The performance of syringe pumps in unsaturated horizontal column experiments. *Soil Sci.*, 154:243-249, 1992.

Brown, G. O. and D. B. McWhorter, Solute transport by a volatile solvent. *J. Contam. Hydrol.*, 5:387:402, 1990.

Bruce, R. R. and A. Klute, The measurement of soil diffusivity. *Soil Sci. Soc. Proc.*, 20:458-462, 1956.

Burdine, N. T., Relative Permeability calculations from pore-size distribution data. *Petr. Trans. AIMME*, 198:71-77, 1953.

Carsel, R. F. and R. S. Parish, Developing joint probability distributions of soil and water retention characteristic. *Wat. Resour. Res.*, 24:755-769, 1988.

Clothier, B. E., D. R. Scotter, and A. E. Green, Diffusivity and one-dimensional absorption experiments. *Soil Sci. Soc. Am. J.*, 47:641-644, 1983.

Conca, J. L. and J. Wright, The UFA method for rapid, direct measurements of unsaturated transport properties in soil, sediment, and rock. *Aust. J. Soil Res.*, 36:291-315, 1998.

Gardner, W. H., Water Content, in *Methods of Soil Analysis, Part 1*, A Klute ed. 2nd edition, Soil Science Society of America, Madison, WI., 1986.

Klute, A., Some theoretical aspects of the flow of water in unsaturated soils. *Soil Sci. Soc. Proc.*, 16:144-148, 1952.

McBride, J. F. and R. Horton, An empirical function to describe measured water distributions from horizontal infiltration experiments. *Wat. Resour. Res.*, 21:1539-1544, 1985.

McWhorter, D. B., Infiltration affected by flow of air. *Hydrology Paper #49, Colorado State University, Fort Collins,* 1971.

Meyer, J. J. and A. W. Warrick, Analytical expression for soil water diffusivity derived from horizontal infiltration experiments. *Soil Sci. Soc. Am. J.,* 54:1547-1552, 1990.

Mualem, Y., A new model for predicting the hydraulic conductivity of unsaturated porous media. *Wat. Resour. Res.,* 12:513-522, 1976.

Philip, J. R., General method of exact solution of the concentration-dependent diffusion equation. *Aust. J. Phys.,* 13:1-12, 1960.

Philip, J. R., Theory of infiltration. *Adv. Hydrosci.,* 5:215-296, 1969.

Philip, J. R., On solving the unsaturated flow equation: 1. The flux concentration relation. *Soil Sci.,* 116:328-335, 1973.

Philip, J. R. and J. H. Knight, On solving the unsaturated flow equation: 3. New quasi-analytical technique. *Soil Sci.,* 117:1-13, 1974.

van Genuchten, M. Th., A closed-form equation for predicting the hydraulic conductivity of unsaturated soils. *Soil Sci. Soc. Am. J.,* 44:892-898, 1980.

van Genuchten, M. Th., F. J. Leij, and S. R. Yates, The RETC Code for Quantifying the Hydraulic Functions of Unsaturated Soils, Version 1.0. *EPA Report 600/2-91/065,* U.S. Salinity Laboratory, USDA, ARS, Riverside, California, 1991.

Warrick, A. W., Soil water diffusivity estimates from one-dimensional absorption experiments. *Soil Sci. Soc. Am. J.,* 58:72-77, 1994.

Warrick, A. W., D. O. Lomen, and S. R. Yates, A generalized solution to infiltration. *Soil Sci. Soc. Am. J.,* 49:34-38, 1985.
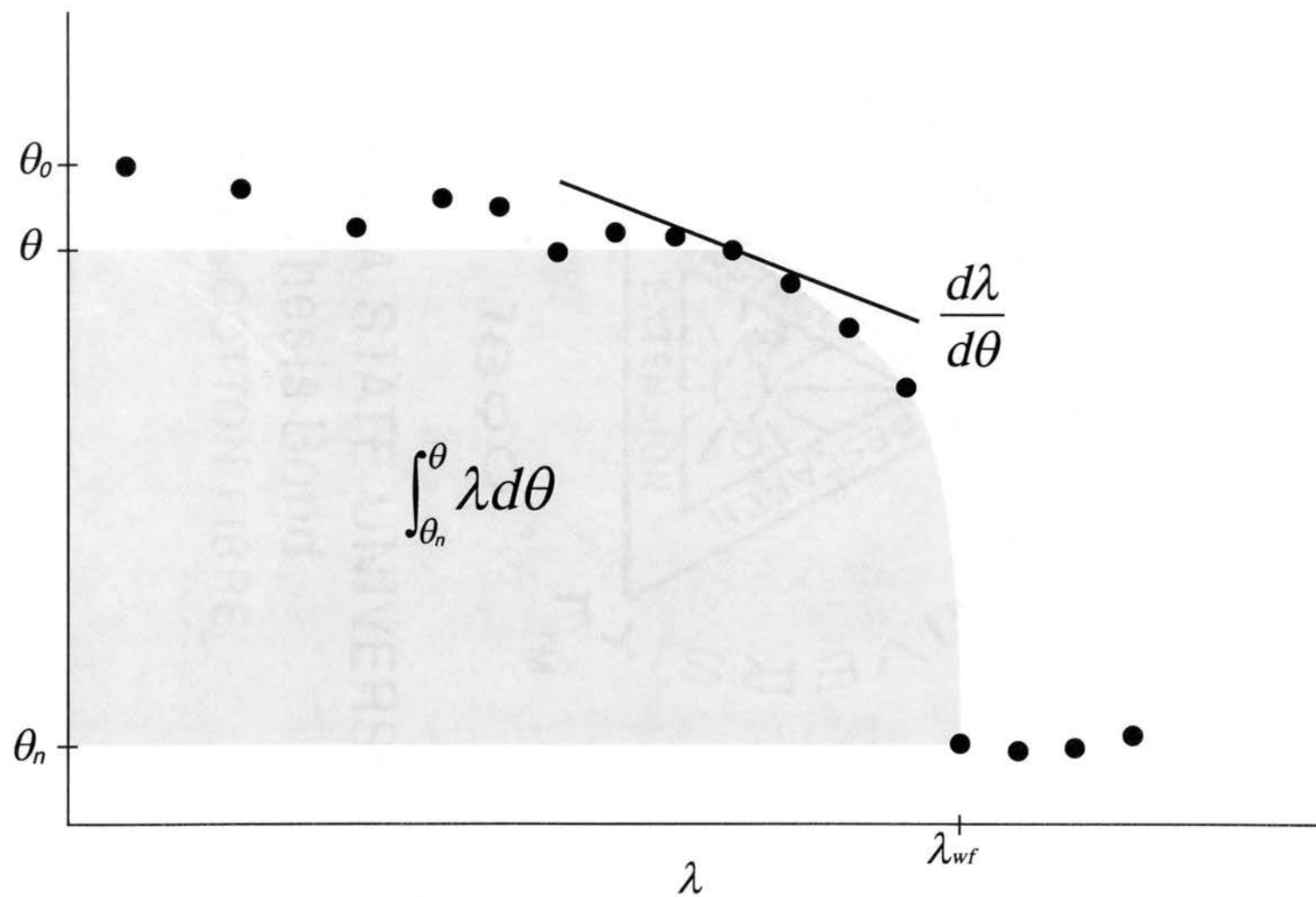
Figure 2-1. Graphical representation of $D(\theta)$ from $\lambda(\theta)$.
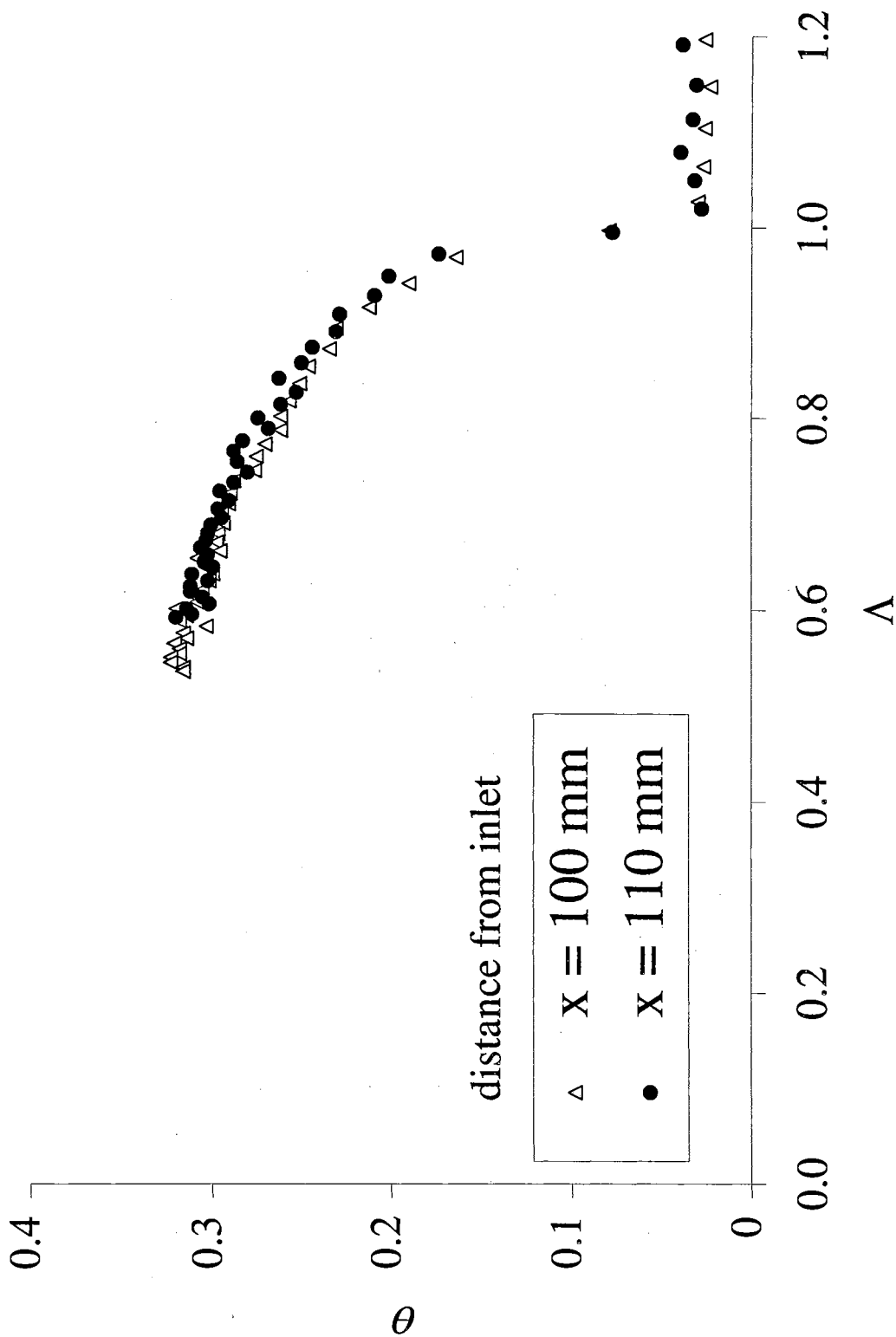
Figure 2-2. Measured $\Lambda(\theta)$.
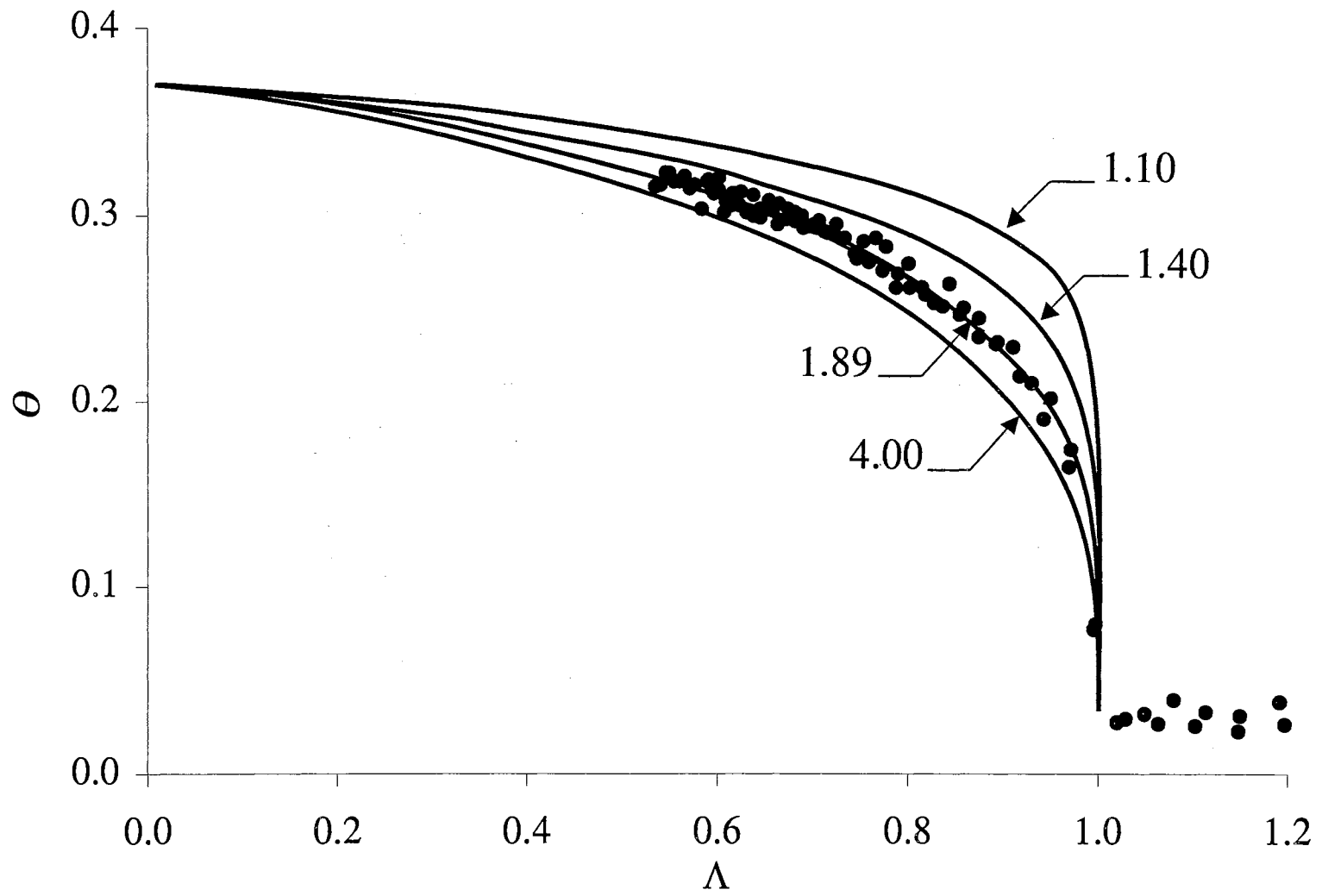
Figure 2-3. Optimization of *n* (various values of *n* shown).
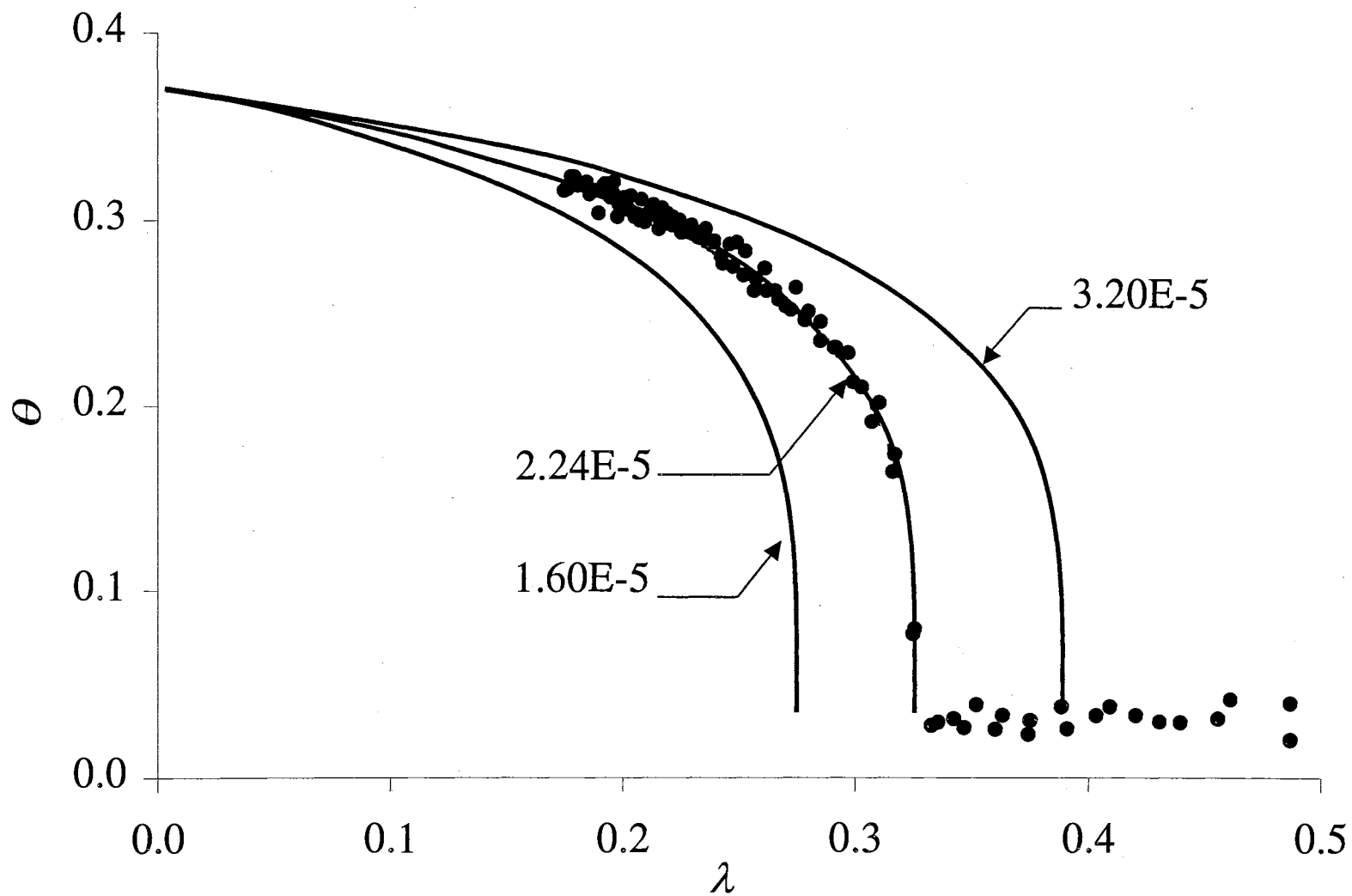
Figure 2-4. Optimization of K_s/α (various values of K_s/α shown).
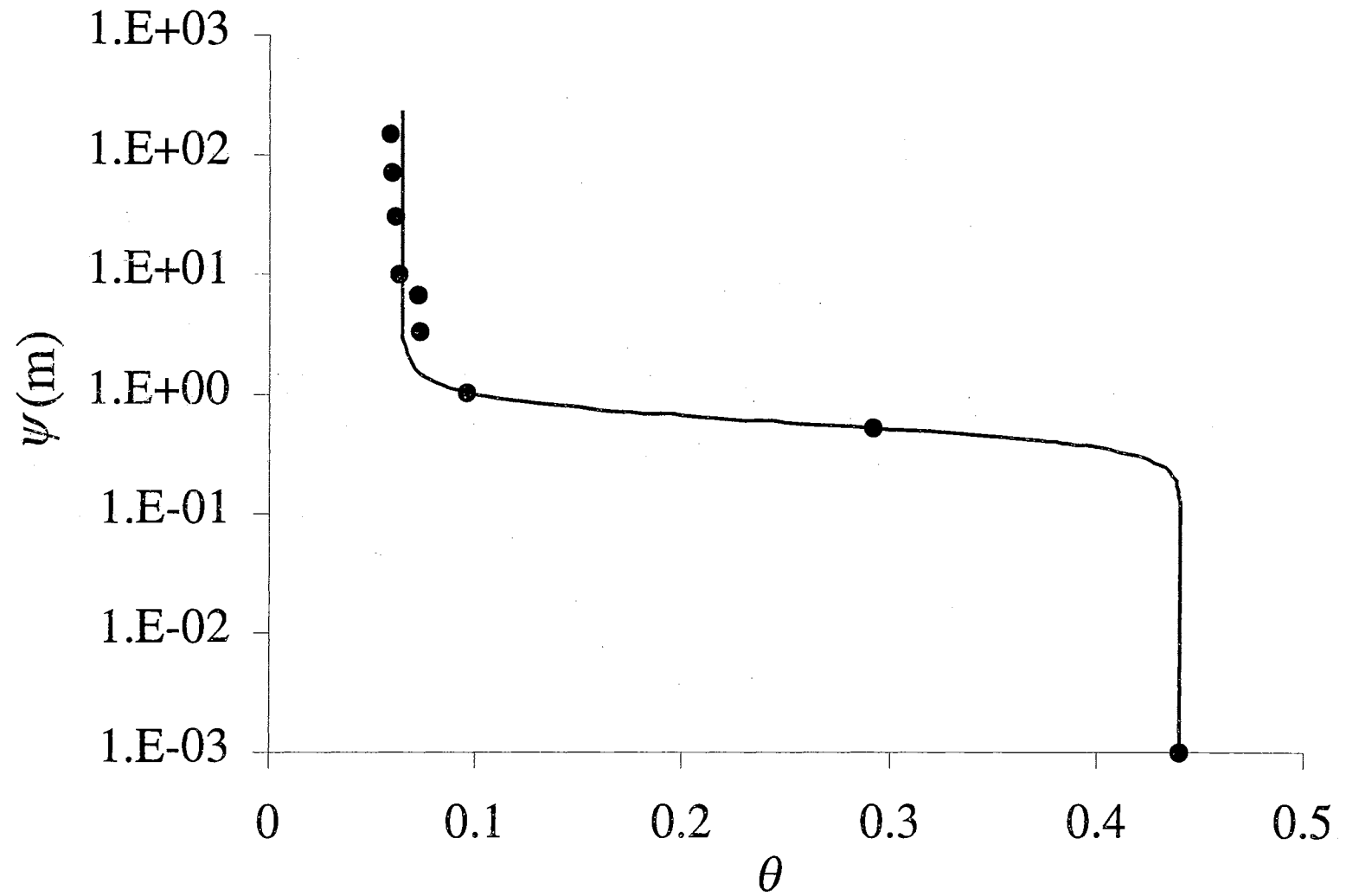
Figure 2-5. Measured $\psi(\theta)$ and fit of (2-1) using RETC.
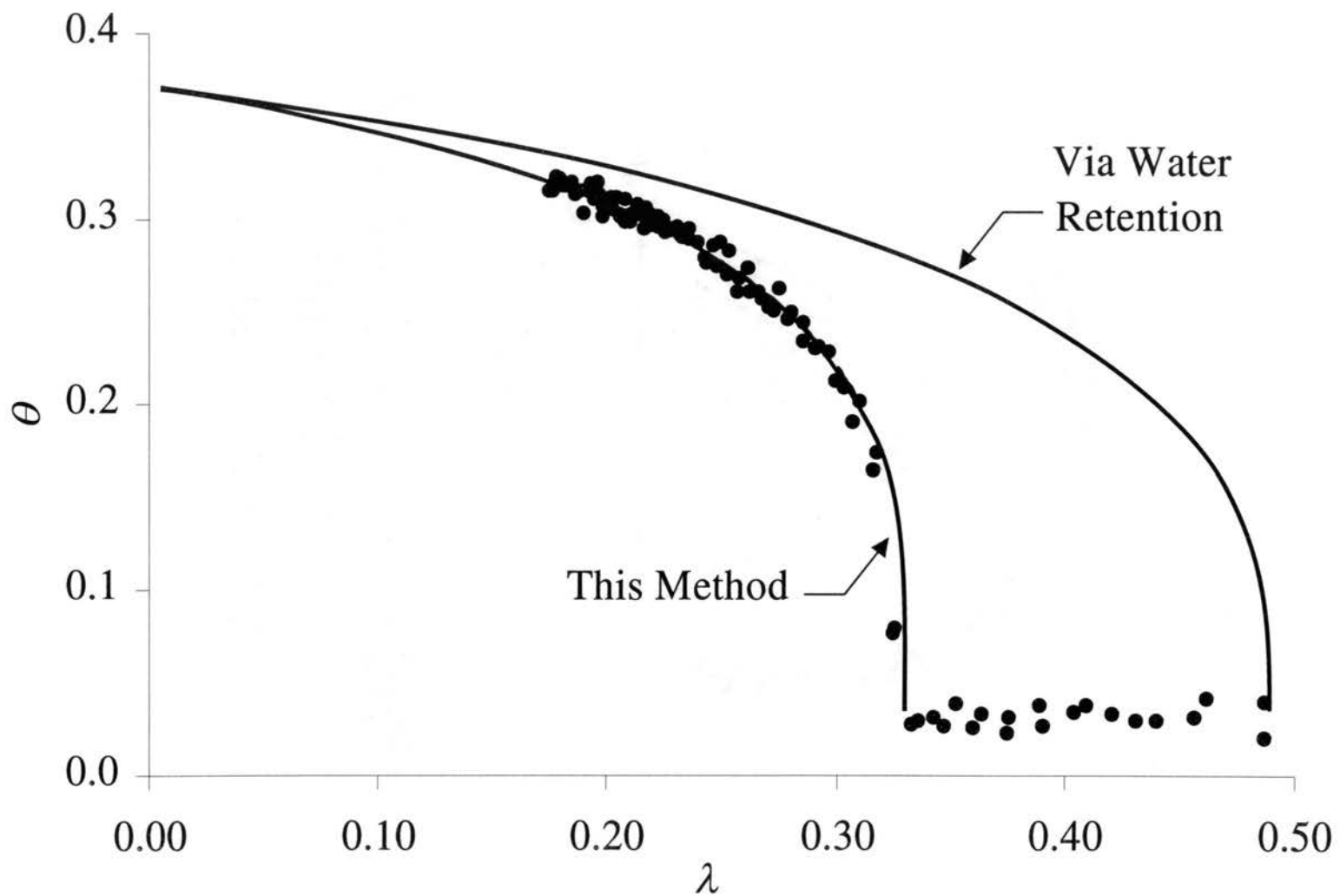
Figure 2-6. Comparison of this method and water retention estimates to measured data.
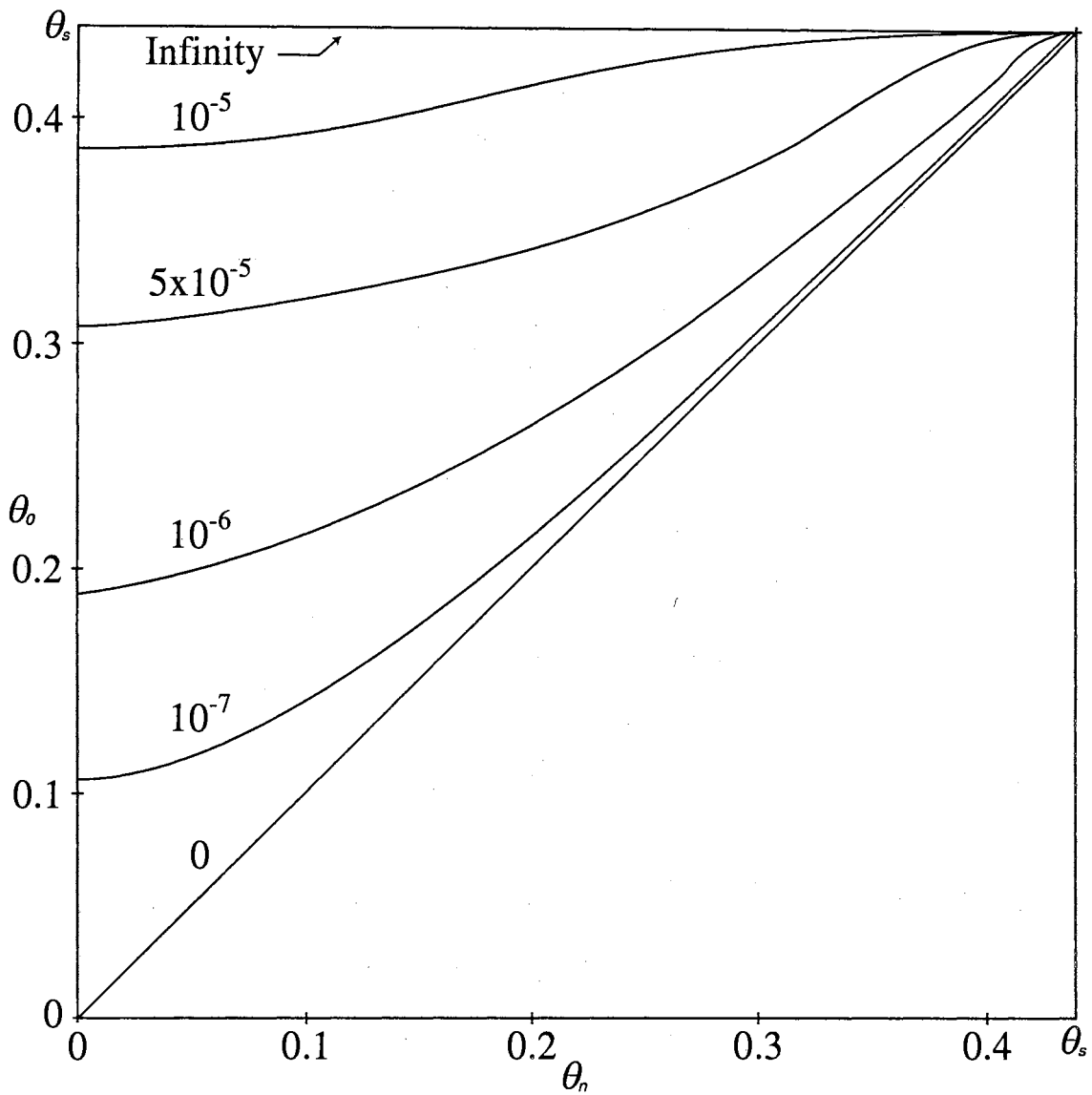
Figure 2-7. Sorptivity as a function of θ_o and θ_n.

CHAPTER III

CHLORIDE MASS BALANCE TO DETERMINE WATER FLUXES BENEATH KCL FERTILIZED CROPS

3.1 Abstract

The utilization of Chloride Mass Balance (CMB) to determine water fluxes has generally been restricted to applications in arid to semi-arid environments, because only in such environments does the chloride deposited by precipitation and dry fallout concentrate sufficiently by evapotranspiration for accurate measurement. This study successfully applied CMB to dryland winter wheat plots with 860 mm of precipitation per year. Soil cores were collected from long-term dryland winter wheat test plots located near Stillwater, OK, which had known, constant applications of the fertilizer KCl for the past 29 years. This additional chloride was sufficient to allow for accurate chloride concentration measurement. Groundwater recharge rates of 12.2 to 38.9 mm/yr were calculated with recharge increasing with fertilizer N. These fluxes may be overestimated by up to 20% based on anion exclusion measurements from adjacent soil cores. Numerical modeling of the chloride distributions beneath the plots supported the assumptions of CMB.

3.2 Introduction

In 1997, Oklahoma winter wheat production covered 5.4 million acres or 58% of the total harvested acreage and 12% of the total state area [*Oklahoma Agricultural*

34

Statistics Service, 1998]. As elsewhere, the threat of nitrate groundwater contamination from fertilizer has been a concern for many years. As part of an effort to estimate the nitrate flux from winter wheat production, Chloride Mass Balance (CMB) was employed to estimate the water flux beneath the root zone. It is assumed all downward water and solute flux beyond the reach of plant roots will ultimately reach the groundwater table. Thus, the mass flux of any conservative solute such as nitrate, may be computed as the product of its soil water concentration and the downward water flux. Nitrate concentrations are relatively easy to measure, however the water flux is difficult to accurately quantify using traditional methods.

A commonly applied method to estimate recharge is a hydrologic water balance, but the evapotranspiration component is difficult to estimate. Also, when recharge is small compared to precipitation a poor evapotranspiration estimate can lead to relatively large errors in computed recharge. Another method to estimate recharge relies on using suction lysimeters to measure soil suction vertically within the unsaturated soil column. Soil suction along with estimates of the unsaturated hydraulic conductivity allows the application of the Buckingham flux law [*Buckingham*, 1907]. Again estimation errors arise in the presence of low recharge rates since the difference in head between lysimeters at varying depths may be relatively small and because hydraulic conductivity is so strongly dependent on the soil suction. Under such conditions a tracer method such as CMB is more promising.

The objectives of this study are to estimate the water flux beneath the root zone of experimental winter wheat plots using CMB, and to verify assumptions of CMB by numerical modeling of the measured field conditions. The estimation of the water flux

allows for the subsequent assessment of the potential for groundwater contamination by nitrates under fertilized winter wheat plots. To this end, 2.5 m deep soil cores were collected from long-term dryland winter wheat (*Triticum aestivum* L.) test plots located near Stillwater, OK. The soil cores were evaluated for water content, bulk density, and chloride concentration at various depths. By equating the chloride mass flux at the surface to the chloride mass flux at depth, CMB provides estimates of the vertical downward water flux beneath the experimental winter wheat plots. Each test plot had identical management for the previous 29 years with the exception of four different nitrogen fertilizer application rates (0, 45, 90, 135 kg/ha/yr of N). The results of different N application are visibly apparent with the zero N application wheat plots being small and yellowish, while the 90 and 135 N application wheat plots are lush and dark green. Utilization of CMB on the four different groups of fertilizer application rate plots allows a comparison of groundwater recharge between healthy and N limited winter wheat crops. The water flux was also numerically modeled for the conditions of the experimental winter wheat plots to help validate assumptions of CMB.

3.3 The Long Term Plots

Long-term winter wheat fertility tests were established at the Oklahoma State University (OSU) Agricultural Research Station in 1969. Since then, continuous dryland winter wheat has been cultivated on 6.1 m by 18.3 m plots in Kirkland clay loam (fine, mixed, thermic Udertic Paleutoll). The plots are located in a topographically high location, which prevents runon. To minimize cross plot contamination, the plots were disked parallel to the plot length and approximately perpendicular to the slope. The area

receives an average of 860 mm of precipitation per year and the groundwater table is at a depth of approximately 5 m. Figure 1 shows typical values for percent sand, percent clay, and bulk density versus depth from soil cores collected in this study. While variations of the particle size distributions with depth are present, no discrete textural layers were discernable by visual inspection. Similarly, textural variations were not constant between cores.

Plots are grouped by fertilizer application rate (A, B, C, and D), with each group having four replications. Treatments and replicate test plots were placed in a random pattern throughout a single field. The test plot groups and corresponding fertilizer application rates are given in Table 3-1. The N, P, and K sources for the sixteen plots are NH_4NO_3 (34-0-0), triple superphosphate (0-20-0), and KCl (0-0-56), respectively [*Raun and Johnson*, 1995].

Table 3-1. Test Plot Fertilizer Treatments

| Plot Groups | Fertilizer Applied 1969 to Present (kg/ha/yr) | | | Grain Yield (1993) |
	N	P	K / Cl	(kg/ha/yr)
A	0	29	38 / 34.4	1480
B	45	29	38 / 34.4	1870
C	90	29	38 / 34.4	1930
D	134	29	38 / 34.4	1970
	Fertilizer Applied 1957 to 1968 (kg/ha/yr)			Grain Yield
A,B,C,D	54	22	0 / 0	Unknown

Prior to the establishment of the winter wheat fertility tests in 1969, the fields were used from 1957 to 1968 for winter wheat production and fertilized as shown at the bottom of Table 3-1. Prior to 1957 the use of the land is unknown, but it is likely that wheat or legumes were grown without fertilization or irrigation after its first cultivation in approximately 1890. Also listed in Table 3-1 are the average grain yields from 1993,

which represent typical current yields for the test plots. The reason winter wheat yield can be sustained with zero N application (Group A plots) has previously been studied on adjacent test plots. In those plots there has been no N fertilization for 100 years and the plant N source is primarily supplied by mineralization of soil organic matter, which has declined from 3.7 to 1.0% by dry weight [*Bowman, et. al.,* 1996].

3.4 Soil Sampling

After the 1997 and 1998 wheat harvests, 67 mm diameter continuous soil cores were collected to a depth of approximately 2.5 m using a hydraulic soil sampler in direct push mode. *Brown et al.* [1994] have previously shown that this sample size and collection method is adequate to describe the density variation of the soil matrix. The cores were cut into 50 mm long samples and then further split longitudinally into two sub-samples. The first sub-sample was used to measure gravimetric moisture content [*ASTM,* 1993]. Soluble pore water extracts were obtained from the second sub-sample using a 1:1 soil-deionized water extract [*Mulvaney,* 1996]. The chloride concentration of the extract was measured by ion chromatography using a Dionex 2000i. Attempts to extract pore water by high-speed centrifugation were generally unsuccessful due to the relatively low water content and high clay content of the samples. Sections of the core not used for other analyses were used to determine bulk density using the Clod Method [*Blake and Hartage,* 1986].

3.5 CMB Theory

CMB has been applied extensively to estimate groundwater recharge in arid regions [*Bresler*, 1973; *Allison et al.*, 1985; *Johnston*, 1987; *Phillips*, 1994; *Tyner*, 1998]. It equates the mass flux of chloride at the ground surface to the mass flux of chloride beneath the depth of evapotranspiration. Chloride is applied naturally at the soil surface from precipitation and dry fallout. Under steady state, 1-D flow, the chloride mass flux at any depth will equal the chloride mass flux at the surface. *Scanlon* [1991] defines the chloride mass flux under steady state conditions by

$$\dot{m} = -D\,dC\!\!\diagup\!\!_{dz} + Cq \tag{3-1}$$

Solving for q yields the volumetric water flux

$$q = \frac{1}{C}\left[\dot{m} + D\frac{dC}{dz}\right] \tag{3-2}$$

where q is the volumetric water flux, C is the pore water chloride concentration, $\dot{m}$ is the chloride mass flux, D is the hydrodynamic dispersion coefficient, and z is the vertical space coordinate. As water moves downward through the soil profile, some of it is removed by evapotranspiration, reducing the water flux and causing the remaining pore water chloride to become increasingly concentrated. Thus, (3-2) is normally applied beneath the root zone where no additional water is removed by evapotranspiration. In arid regions, it is often assumed that D is negligible [*Allison et al.*, 1985, *Phillips*, 1994] and (3-2) simplifies to

$$q = \dot{m}\!\!\diagup\!\!C \tag{3-3}$$

The pore water age at a given depth can be calculated by dividing the mass of chloride in the profile above that depth by the surface chloride mass flux

$$t_z = \frac{\int_0^z \theta C dz}{\overset{\bullet}{m}} \qquad (3\text{-}4)$$

where t_z is the pore water age at a depth of z and θ is the volumetric moisture content [*Phillips*, 1994].

In this study the sum of chloride from fertilizer and precipitation minus the chloride removed by harvesting was used to determine the net amount of chloride applied to the plots annually. The primary source of chloride for the test plots was an annual application of KCl that added 34.4 kg/ha/yr of chloride. Precipitation added approximately 1.65 kg/ha/yr of chloride [*NADP/NTN*, 1983]. Precipitation input was estimated by multiplying the average precipitation chloride concentration with the annual precipitation rate. Crop harvesting resulted in losses of 0.8 to 1.1 kg/ha/yr of chloride. These losses were calculated by multiplying the chloride concentration in the wheat grain [*Engel et al.*, 1998] by the annual wheat grain harvest. Normally CMB is only applied in arid and semi-arid regions that exhibit very low groundwater recharge (i.e. high chloride concentrations). In areas with higher recharge rates, the chloride concentration is generally too low to be measured accurately. We were able to apply CMB in this sub-humid area with 860 mm of precipitation per year [*Myers*,1982] because of the relatively large amount of chloride that was artificially added by fertilization.

3.6 CMB Assumptions

Assumptions of CMB include: 1) vertical downward piston displacement adequately represents the chloride transport (i.e. little to no preferential flow), 2) chloride is not retarded by adsorption nor accelerated by anion exclusion, 3) chloride is conservative, 4) chloride application rate is constant and known, 5) there is no appreciable runon or runoff from the sampling sites, and 6) steady state conditions prevail in the soil column [*Johnston*, 1987; *Dettinger*, 1989; *Scanlon* 1992; *USGS*, 1994; *Ginn and Murphy*, 1997].

3.61 Assumption 1

Violation of assumption 1 can occur at two scales, a small scale (smaller than the sample size), and a large scale (larger than the sample size). If preferential flow occurs at a small scale, CMB will yield a result equal to the volumetrically weighted harmonic mean of the individual water fluxes within the sample measured. This can be shown with the knowledge that pore water extracted from a soil sample by dilution results in a chloride concentration of

$$C = \frac{\sum_{i=1}^{n} \theta_i F_i C_i}{\sum_{i=1}^{n} \theta_i F_i} \qquad (3\text{-}5)$$

where θ_i and C_i are the volumetric water content and pore water chloride concentration of the ith flowpath within the sample respectively, and F_i is the volume of the ith flowpath within the sample divided by the total volume of the sample. Substituting (3-5) into (3-3) results in

41

$$q_{CMB} = \frac{\dot{m} \sum_{i=1}^{n} \theta_i F_i}{\sum_{i=1}^{n} \theta_i F_i C_i} \qquad (3\text{-}6)$$

where q_{CMB} is the water flux calculated using CMB. Assuming that $\dot{m}$ is constant across an area and no mixing between flow paths occurs, then (3-3) can be inverted and generalized to show

$$C_i = \dot{m} \big/ q_i \qquad (3\text{-}7)$$

where q_i is the water flux of the ith flowpath.

Substituting (3-7) into (3-6) results in

$$q_{CMB} = \frac{\sum_{i=1}^{n} \theta_i F_i}{\sum_{i=1}^{n} \frac{\theta_i F_i}{q_i}}, \qquad (3\text{-}8)$$

which is equivalent to the volumetrically weighted harmonic mean of the fluxes within the sample. The actual water flux of the sample, q_A, is of course equal to the total of the flowpaths

$$q_A = \sum_{i=1}^{n} F_i q_i = \dot{m} \sum_{i=1}^{n} \frac{F_i}{C_i} \qquad (3\text{-}9)$$

where the right hand side of (3-9) results from the substitution of (3-7).

As an example of the error associated with small-scale preferential flow, if a soil sample has two flowpaths, the first with $\theta_1 = 0.15$, $F_1 = 0.2$, and $C_1 = 100\,\text{mg/l}$, and the other with $\theta_2 = 0.45$, $F_2 = 0.8$ and $C_2 = 200$ mg/l, applying (3-6), CMB will calculate $q_{CMB} = 192\,\text{mg/l}$. The true flux through the sample is calculated using (3-9) and results in

$q_A = \dot{m}/167$ mg/l. Thus, q_{CMB} is 13% smaller than q_A in this example. q_{CMB} will always be less than q_A unless all of the q_i are equal in which case q_{CMB} will be equivalent to q_A. However, if the intent is to calculate the water flux, q_{CMB} is a useful estimate and the error associated with using q_{CMB} versus q_A may be small relative to other experimental errors. Difficulties can arise if the preferential flow takes place through large macropores which may not contain water and chloride during the time of sampling [*Wood*, 1999]. Given the clay loam soil, the moisture contents of the test plots (approximately 0.28), and a visual inspection of the cores, macropores and thus macropore flow do not seem likely beneath an appreciable depth.

If preferential flow occurs on a scale larger than the sample size, the fluxes calculated are accurate, but they can not be extrapolated without consideration of the large-scale variability. Indication of large-scale preferential flow is evidenced by a large coefficient of variation for the measured water fluxes between cores.

Lastly, although it is often stated that an assumption of CMB is vertical flow, this is not strictly required. A more precise statement is that CMB measures the vertical component of flow within a porous media. As long as the flow has some vertical downward component, CMB results will be an estimate of that vertical component of flow.

3.62 Assumption 2

Chloride ions often experience anion exclusion because most soils have a negative charge. Applying CMB to a soil that exhibits anion exclusion results in a measured water flux that is greater than the true water flux. Chloride in clay rich soils

has been measured traveling at velocities up to twice as high as the corresponding water velocities [*Gvirtzman et al.*, 1986]. In a similar nearby soil, *Brown and Allred* [1993] found that anions traveled up to 20% faster than corresponding water velocities which would result in a potential overestimate of groundwater recharge using CMB by the same amount. Since both chloride and nitrate have a similar charge they generally behave similarly in regards to anion exclusion. Thus, the estimate of water flux based on chloride is appropriate for the ultimate goal of estimating nitrate flux even if minor anion exclusion is occurring.

3.63 Assumption 3

Chloride is assumed to be conservative based on a history of use as a tracer and *Hem's* [1985] statement:

> "Chloride ions do not significantly enter into oxidation or reduction reactions, form no important solute complexes with other ions unless the chloride concentration is extremely high, do not form salts of low solubility, are not significantly adsorbed on mineral surfaces, and play few vital biochemical roles. The circulation of chloride ions in the hydrologic cycle is largely through physical processes."

Since the measured chloride concentrations are not high, the assumption of conservative behavior appears valid.

3.64 Assumption 4

Assumption 4 has historically been the most problematic because data describing the amount of chloride present in precipitation and dry fallout is difficult to obtain. Another problem is that if a soil column represents a long time period of infiltration, it is difficult to determine if the environmental conditions at the site have been temporally consistent with the measured chloride input data [*Edmunds and Gaye*, 1994; *Murphy et al.*, 1996; *Love et al.*, 2000]. Since the artificially applied chloride, in the form of KCl, makes up approximately 95% of the chloride added to the plots over the last 29 years, the difficulty of estimating atmospherically deposited chloride becomes relatively insignificant.

3.65 Assumption 5

The single annual fertilizer application, which represents a relatively large percentage of total chloride added to the plots, strengthens the assumption that significant amounts of chloride will not be added or lost from the plots by runon or runoff. Since KCl is highly soluble and applied only once a year, it would take a very strong precipitation event just after fertilization to wash away the KCl before it could be dissolved and infiltrate into the upper soil column, which is a very unlikely scenario. Runon or runoff of water thus will only be at rainfall chloride concentrations, which is relatively insignificant to the total chloride mass balance.

At a time scale of weeks or months water flux rates are mostly in an unsteady state because weather and agricultural practices changes throughout the year. However, over a time scale of years, the test plots are believed to be in a pseudo steady state condition.

3.7 Numerical Modeling

Numerical modeling was carried out using Hydrus 1-D version 7.0 [1998] to determine if the application of uniform 1-D transport and reasonable values for the transport parameters could accurately reproduce the water and chloride transport through the soil profile. The numerical model solves the Richards equation for one-dimensional transport of water, heat, and multiple solutes in variably saturated media while including a sink term to account for water uptake by plant roots. An initial model time step of 0.1 days with a maximum of 1 day was used for a duration of 29 years. The upper boundary was modeled with a constant flux rate equal to the average precipitation rate of 860 mm/yr and a chloride concentration equaling the net annual chloride applied to the plots divided by the annual precipitation. This is an acceptable simplification due to the low transport rates of water and solutes within the fine textured soil. The lower boundary was modeled with a zero hydraulic gradient and constant chloride concentration flux at a depth adequate to preclude an influence on the simulation.

Initial modeling was conducted using Hydrus's default hydrologic parameter values for a typical clay loam soil. These hydrologic values included Van Genuchten's soil water retention parameter (α), soil water retention exponent (n), and saturated

hydraulic conductivity (K_s). Root water uptake versus depth was calibrated to achieve the measured chloride concentrations within the root zone. Next α, n, and K_s were calibrated to provide the measured volumetric water content throughout the soil column. Finally, the dispersivity was estimated by optimizing the fit of the modeled chloride dispersion ahead of the chloride bulge to measured values. Although dispersion was included in the model, the results section will explain why D is assumed to be negligible in regards to the water flux calculations of (3-2).

3.8 Results

3.81 Measured Chloride Profiles

Measured chloride concentrations varied from plot to plot making the true signal sometimes difficult to recognize. For this reason, the mean and 90% confidence intervals of the chloride concentrations were plotted versus depth for plot groups A, B, C, and D in Figures 2, 3, 4, and 5, respectively. The confidence intervals were plotted assuming a normal distribution. Every depth of every group was considered its own population so there were a maximum of eight points per population. As a result of the small number of points per depth, the true distribution could not be found directly and the normal confidence intervals that are shown may contain error resulting from the choice of the distribution.

The group A data (Figure 2) show a well-defined chloride bulge. This bulge is only present because the bottom of the system has not reached steady state in regards to the additional chloride flux since 1969. A pseudo steady state condition has been achieved throughout the root depth as will be shown in the modeling section. Given

sufficient time, the chloride concentration would be expected to reach a relatively constant value beneath the root depth at approximately 0.8 m. Chloride profiles for Group B and C test data (Figure 3 and 4) are similar to a depth of about 2 m. Beneath this depth the chloride content of the Group C test data seems to increase dramatically. This apparent increase must be tempered with the knowledge that the higher mean chloride concentrations beneath a depth of 2 m are described by fewer samples due to the difficulty in collecting intact cores to such depths. A possible mechanism to obtain such high chloride concentrations beneath 2 m may be associated with the prairie conditions present prior to initial cultivation as discussed in the next section. The chloride profiles for group B and C test data also show a deeper root depth, approximately 1.25 m, than the Group A test data. Since the Group A plots have received zero N as NH_4NO_3 over the past 29 years, it is plausible that being nitrogen limited has restricted the root growth below 0.8 m in the Group A plots.

Shallow chloride concentrations for group D test data (Figure 5) are lower than the concentrations in the other plots, which correlates to a higher water flux. The chloride gradient is especially small in the upper 0.6 m. It is possible that the strong vegetative growth due to larger NH_4NO_3 applications may provide an improved surface soil structure and increased surface infiltration.

3.82 Water Fluxes

Table 3-2 presents the mean and standard deviation (SD) of the chloride concentration at the root depth and its associated water flux from (3-3). The mean water fluxes were calculated from chloride data of individual cores, not the averaged chloride

48

data (Figures 3-4 to 3-7). These fluxes may be overestimated by up to 20% based on anion exclusion measurements from adjacent soil cores. The estimates of water flux are the only regional long-term dryland winter wheat recharge estimates available in the literature with the exception of *Berg et al.* [1991]. Berg measured 3 to 25 mm/yr of recharge, which is consistent with the present water flux estimates, beneath winter wheat fields in northwestern Oklahoma that average 690 mm/yr of precipitation. In his study Berg also found that replacing the native mixed grasslands with terraced winter wheat increased the recharge enough to cause salt seeps in adjacent low lying areas. Lower recharge rates present before initial cultivation in the area currently occupied by the Stillwater test plots may explain the high chloride concentrations seen beneath a depth of 2 m within the Group C test data.

Table 3-2. Chloride Concentrations and Fluxes Calculated Using CMB

Group	Number of Cores		Cl Bulge (mg/l)	Water flux (mm/yr)
A	8	Mean	295	12.2
		SD	62.6	2.6
B	8	Mean	219	17.0
		SD	63.4	5.2
C	7	Mean	173	25.4
		SD	93.9	13.6
D	8	Mean	137	38.9
		SD	101	25.1

It is interesting that as the NH_4NO_3 application rate increases from the Group A plots to the Group D plots, apparently so does the sample mean water flux. The hypothesis that water fluxes from each plot group have identical population distribution functions was tested using the Kruskal-Wallis test [*Conover*, 1980]. At the 90% level of confidence the hypothesis is accepted, but at a more rigorous 75% level of confidence the

hypothesis is rejected. It is therefore likely that the water fluxes between different plot groups are from different populations. We are uncertain of the cause of the differences in water fluxes between plot groups. Again, higher N application produces noticeably more vigorous plants, that in turn, may provide an improved surface soil structure with greater infiltration and less runoff. However, the denser plant stands should also produce greater transpiration, thus reducing net groundwater recharge.

3.83 Modeling

Hydrologic parameters used to model the water fluxes and chloride concentrations are given in Table 3-3. The measured chloride concentrations, modeled chloride concentration at 28 or 29 years (1997 and 1998 samples, respectively), 200 years, and pore water age calculated from (3-4), were plotted for two of the cores (Figure 6 and 7). Two hundred years was arbitrarily chosen as a time period to represent steady state conditions throughout the soil columns. For simplicity, all 28 and 29 years modeling results will be referred to as 29 years for the remainder of the paper.

Table 3-3. Model Simulation Input Parameters

Core	α (1/mm)	N	K_s (mm/d)	Dispersivity (mm)	Porosity	Residual Saturation	Bulk density (g/cm^3)
A-1-98	0.0019	1.25	62.4	110	0.41	0.095	1.7
A-4-97	0.0019	1.20	62.4	30	0.41	0.095	1.7

The modeled chloride bulges at 29 years match the measured chloride data quite well. This is significant since measured and modeled water contents were also maintained. Therefore the known mass of chloride applied over the past 29 years has

been measured in the field and modeled using CMB assumptions with reasonable values for soil hydraulic parameters. Notice also that the pore water ages at the base of the chloride bulges are reasonably close to 29 years, the period of KCl application. This agreement again shows conservation of chloride mass using CMB assumptions. Calibrating hydraulic parameters to fit the modeled data with the measured data does not ensure that the model parameters are accurate, but it does strengthen the argument that at least two of CMB assumptions, no preferential flow and no significant loss of chloride in runoff, are valid. More importantly, it verifies the general shape of the chloride concentration curve created by the addition of KCl for 29 years.

The simplification of (3-2) to (3-3) by excluding D was supported by comparing the maximum concentrations of the modeled chloride concentrations at 29 years and 200 years. At 29 years the modeled chloride pulse has not reached equilibrium beneath the root depth and displays a large chloride concentration gradient. At 200 years the modeled chloride pulse is at equilibrium and no chloride concentration gradient exists below the root depth. Since the root depth chloride concentration at 29 years matches the root depth chloride concentration at 200 years, both the 29 and 200 year simulations will yield similar water fluxes at the root depth using (3-3). In other words, even when a chloride gradient beneath the root zone exists (29 years), the calculated water flux is similar to when a gradient does not exist (200 years). Therefore, at a 29 year time scale D is negligible and the simplification from (3-2) to (3-3) is justified. The similarities in maximum modeled chloride concentrations between 29 and 200 years also strongly imply that the plots have reached a pseudo steady state condition to the base of the root depth during the 29 years of the KCl application.

3.9 Conclusions

Net annual groundwater recharge under dryland winter wheat in Oklahoma was estimated using CMB and duplicated with numerical modeling using CMB assumptions. Both CMB and modeling provided a consistent interpretation of the measured data. The success of the CMB application was due in large part to accurate knowledge of the chloride applied as KCl fertilizer over the last 29 years. Confidence in the results is also a consequence of the site, where the low recharge rates and the large water-holding capacity of the fine textured soil kept all applied chloride within the measured soil profile. Application of fertilizer chloride allowed the chloride input, arguably the most difficult parameter to estimate in a typical CMB application, to be calculated with more certainty. The ability to achieve chloride mass balance while numerically modeling the measured chloride concentration profiles is consistent with the hypothesis that assumptions required for application of the CMB were met. Recharge rates under dryland winter wheat ranged from 12.2 to 38.9 mm per year and increased with increasing N fertilizer application. These fluxes may be overestimated by up to 20% based on anion exclusion measurements from adjacent soil cores. A possible cause for the correlation between water flux and N applied is that the more vigorous plants produced by the higher N rates created a soil structure with greater infiltration and less runoff.

3.10 References

Allison, G. B., W. J. Stone, and M. W. Hughes, Recharge in karst and dune elements of a semi-arid landscape as indicated by natural isotopes and chloride. *J. Hydrol.*, 76:1-26, 1985.

ASTM, Standard test method for laboratory determination of water (moisture) content of soil and rock. *ASTM Standards on Soil Compaction*, D2216-92:52-55, 1993.

Berg, W. A., J. W. Naney, and S. J. Smith, Salinity, nitrate, and waste in rangeland and terraced wheatland above saline seeps. *J. Environ. Qual.*, 20:8-11, 1991

Blake, G. R. and K. H. Hartage, Bulk density, in *Methods of Soil Analysis, Part 1*, A Klute ed. 2nd edition, Soil Science Society of America, Madison, WI., 1986.

Bowman, R. K., S. L. Taylor, W. R. Raun, G. V. Johnson, D. J. Bernardo, L. L. Singleton, The Magruder plots – a century of wheat research in Oklahoma. Dept. of Agronomy, Oklahoma State University, Stillwater, OK., 1996

Brown, G. O. and B. Allred, Anion transport in dry soils. The 1993 Fall Meeting Supplement, EOS, Transactions, American Geophysical Union, 74:297, 1993.

Brown, G. O., M. L. Stone, J. E. Gazin, and S. R. Clinkscales, Gamma ray tomography measurements of soil density variations in soil cores. in *Tomography of Soil-Water-Root Processes*. S. H. Anderson and J. W. Hopmans Ed. SSSA Special Publication 36. Soil Science Society of Amer. Madison, WI., 1994.

Bresler, E., Simultaneous transport of solutes and water under transient unsaturated flow conditions. *Water Resour. Res.*, 9:975-986, 1973.

Buckingham, E., Studies on the movement of soil moisture. *Bureau of Soils Bulletin 38*, Washington D.C., U.S. Dept. of Ag., 1907.

Conover, W. J., *Practical Nonparametric Statistics 2nd Ed.* 229-231, 1980.

Dettinger, M. D., Reconnaisance Estimates of natural recharge to desert basins in Nevada, U.S.A., by using chloride-Balance Calculations. *J. Hydrol.*, 106:55-78, 1989.

Edmunds, W. M. and C. B. Gaye, Estimating the spatial variability of groundwater recharge in the Sahel using chloride. *J. Hydrol.*, 156:47-59, 1994.

Engel, R. E., P. L. Bruckner, and J. Eckhoff. 1998. Critical tissue concentration and chloride requirements for wheat. *Soil Sci. Soc. Am. J.*, 62:401-405.

Ginn, T. R. and Murphy, E. M., A transient flux model for convective infiltration: forward and inverse solutions for chloride mass balance studies. *Water Resour. Res.*, 33:2065-2079, 1997.

Gvirtzman, H., D. Ronen, and M. Magaritz, Anion exclusion during transport through the unsaturated zone. *J. Hydrol.*, 87:267-283, 1986.

Hem, J. D., *Study and interpretation of the chemical characteristics of natural water (3rd ed.)*. USGS Water-Suppl Pap. 2254:264, 1985.

Hydrus, Golden CO.:International Ground Water Modeling Center. Software Package for Simulating the One-Dimensional Movement of Water, Heat and Multiple Solutes in Variably Saturated-Media Ver. 2.0, pp. 1-178. Golden CO.:Colorado School of Mines, 1998.

Johnston, C. D., Distribution of environmental chloride in relation to subsurface hydrology. *J. Hydrol.*, 94:67-88, 1987.

Love, A. J., A. L. Herczeg, L. Sampson, R. G. Cresswell, and L. K. Fifield, Sources of chloride and implications for ^{36}Cl dating of old groundwater, southwestern Great Artesian Basin, Australia. *Water Resour. Res.*, 36:1561-1574, 2000.

Mulvaney, R. L., Nitrogen -- Inorganic Forms. In *Methods of Soil Analysis*: Part 3 Chemical Methods. Ed. J.M. Bigham, Soil Science Society of America No. 9. Chap. 38, Madison WI., 1996.

Murphy, E. M., T. R. Ginn, and J. L. Phillips, Geochemical estimates of paleorecharge in the Pasco Basin: Evaluation of the chloride mass balance technique. *Water Resour. Res.*, 32:2853:2868, 1996.

Myers, H. R., *Climatological Data of Stillwater Oklahoma*. Agricultural Experiment Station Research Report P-281, 1982.

NADP/NTN, *NADP/NTN Data Report Precipitation Chemistry*. Natural Resource Ecology Laboratory. Colorado State University, 1983.

Oklahoma Agricultural Statistics Service, *Oklahoma Agricultural Statistics 1997*. Oklahoma Department of Agriculture. Oklahoma City, OK., 1998.

Phillips, F. M., Environmental tracers for water movement in desert soils of the American southwest. *Soil Sci. Soc. Am. J.*, 58:15-24, 1994.

Raun, W. R. and G. V. Johnson, Soil-plant buffering of inorganic nitrogen in continuous winter wheat. *Agron. J.*, 87:827-834, 1995.

Scanlon, B. R., Evaluation of moisture flux from chloride data in desert soils. *J. Hydrol.*, 128:137-156, 1991.

Scanlon, B. R., Moisture and solute flux along preferred pathways characterized by fissure sediments in desert soils., *J. Cont. Hydrol.*, 128:137-156, 1992.

Tyner, J. S., *Inter-pore Bypass of the Chloride Mass Balance Technique*. M.S. Thesis. San Diego State University. Dis. Abs. No. TD426.T96 1998, 1998.

USGS, *Estimates of Percolation Rates and Ages of Water in Unsaturated Sediments at Two Mojave Desert Sites, California-Nevada*, Rep. 94-4160, 1994.

Wood, W. W., Use and misuse of the chloride-mass balance method in estimating ground water recharge. *Groundwater*, 137:2-3, 1999.
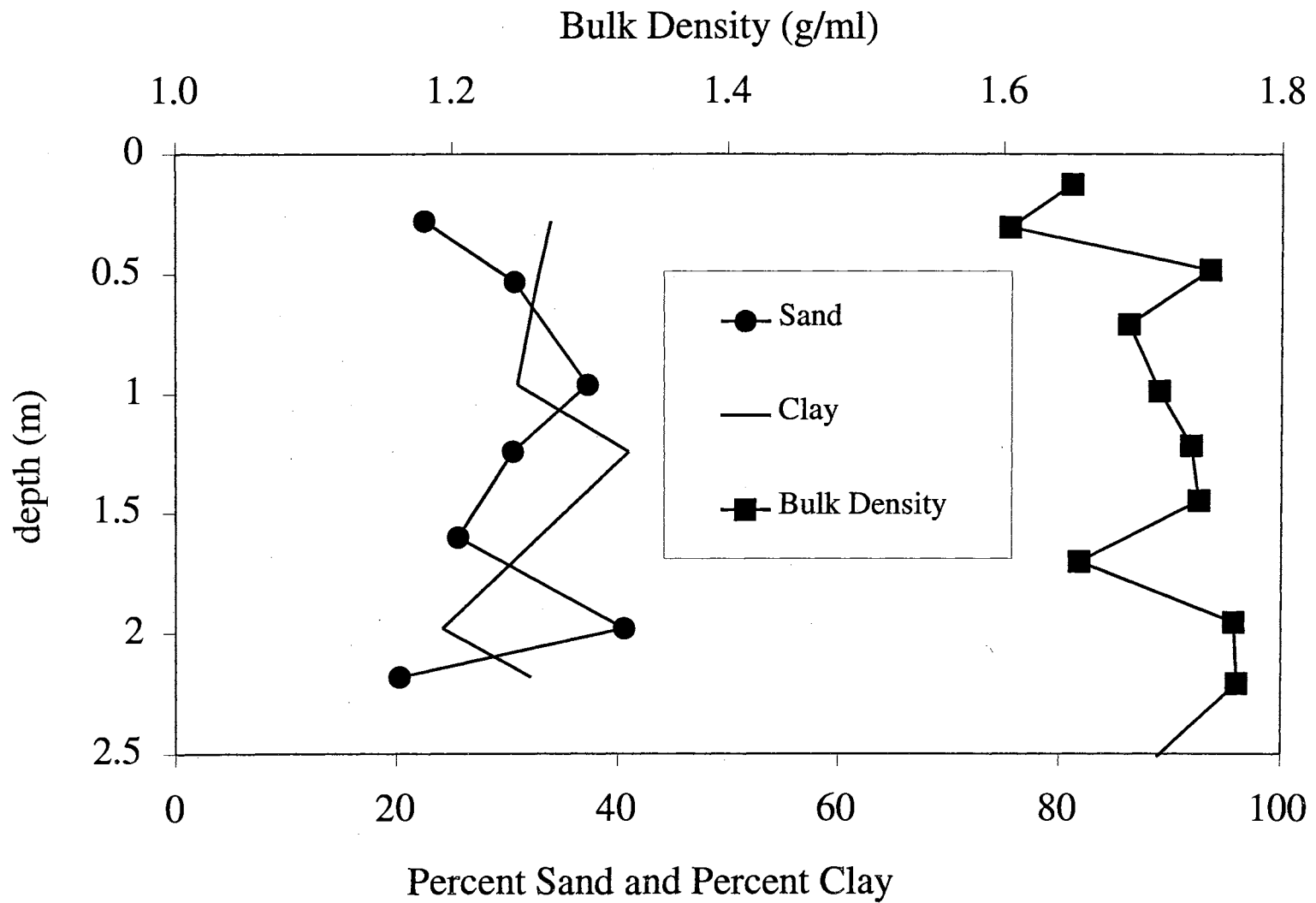
Figure 3-1. Typical soil texture and bulk density.
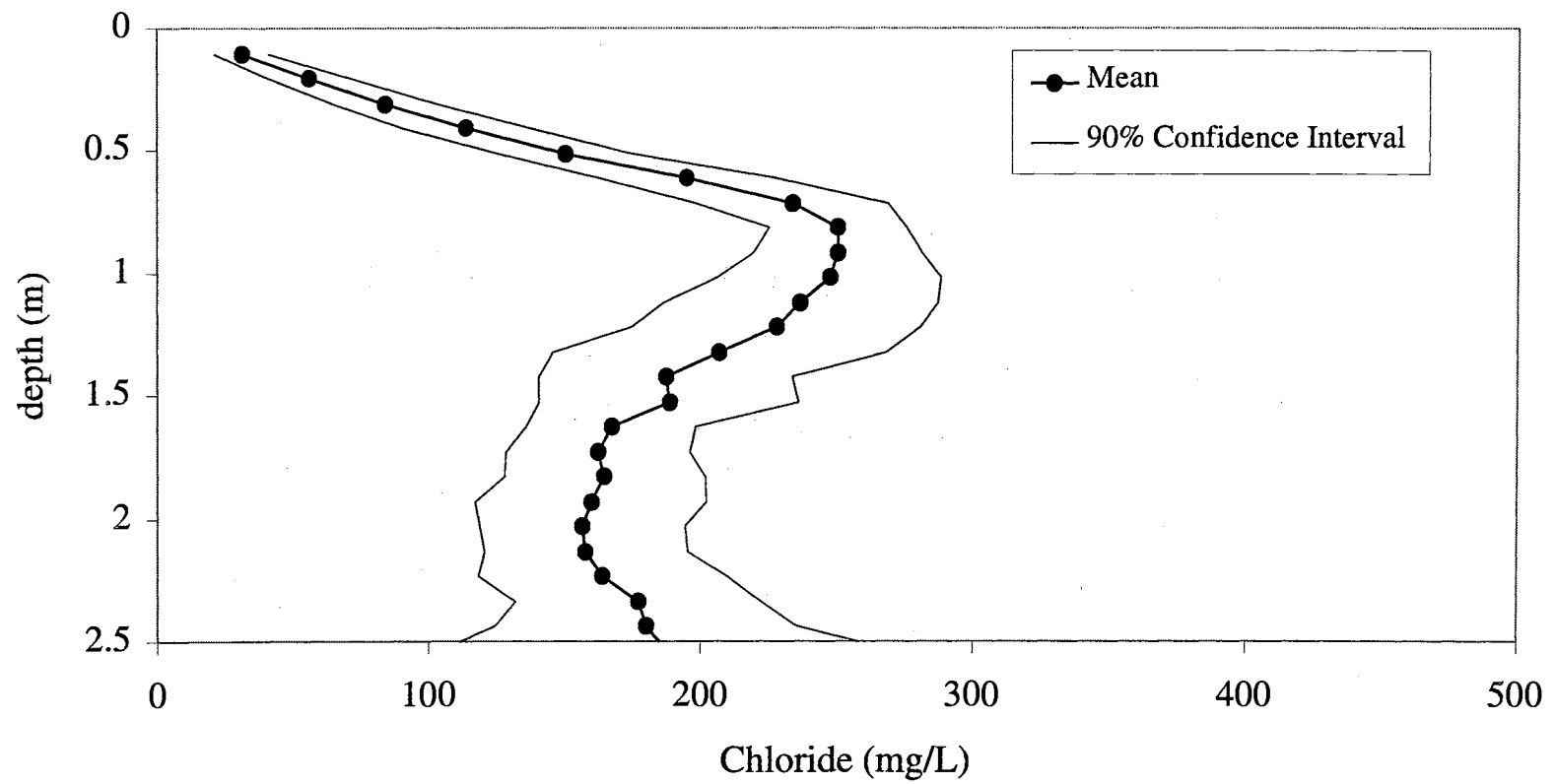
Figure 3-2. Sample mean and 90% confidence intervals of population mean for chloride concentrations of Group A cores.
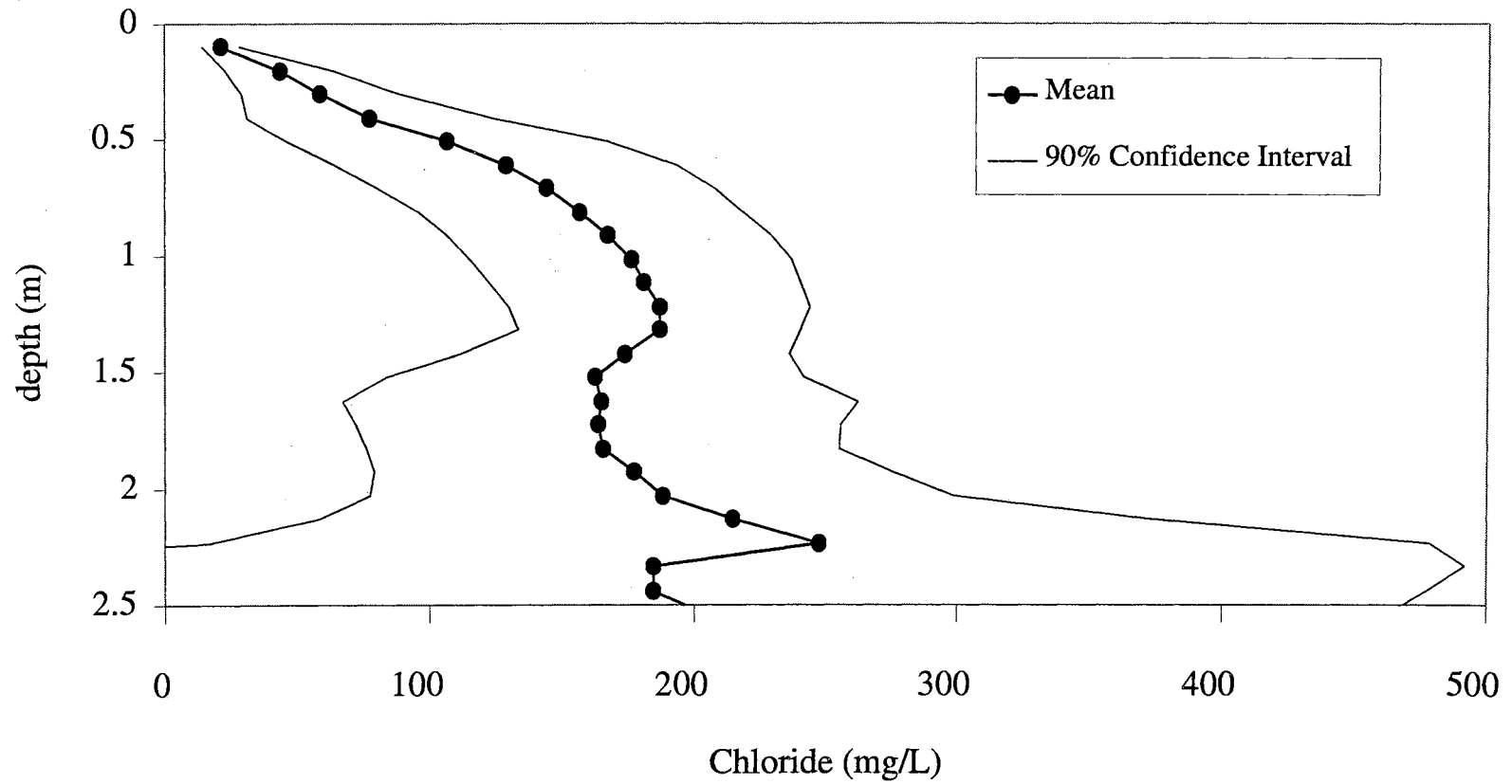
Figure 3-3. Sample mean and 90% confidence intervals of population mean for chloride concentrations of Group B cores.
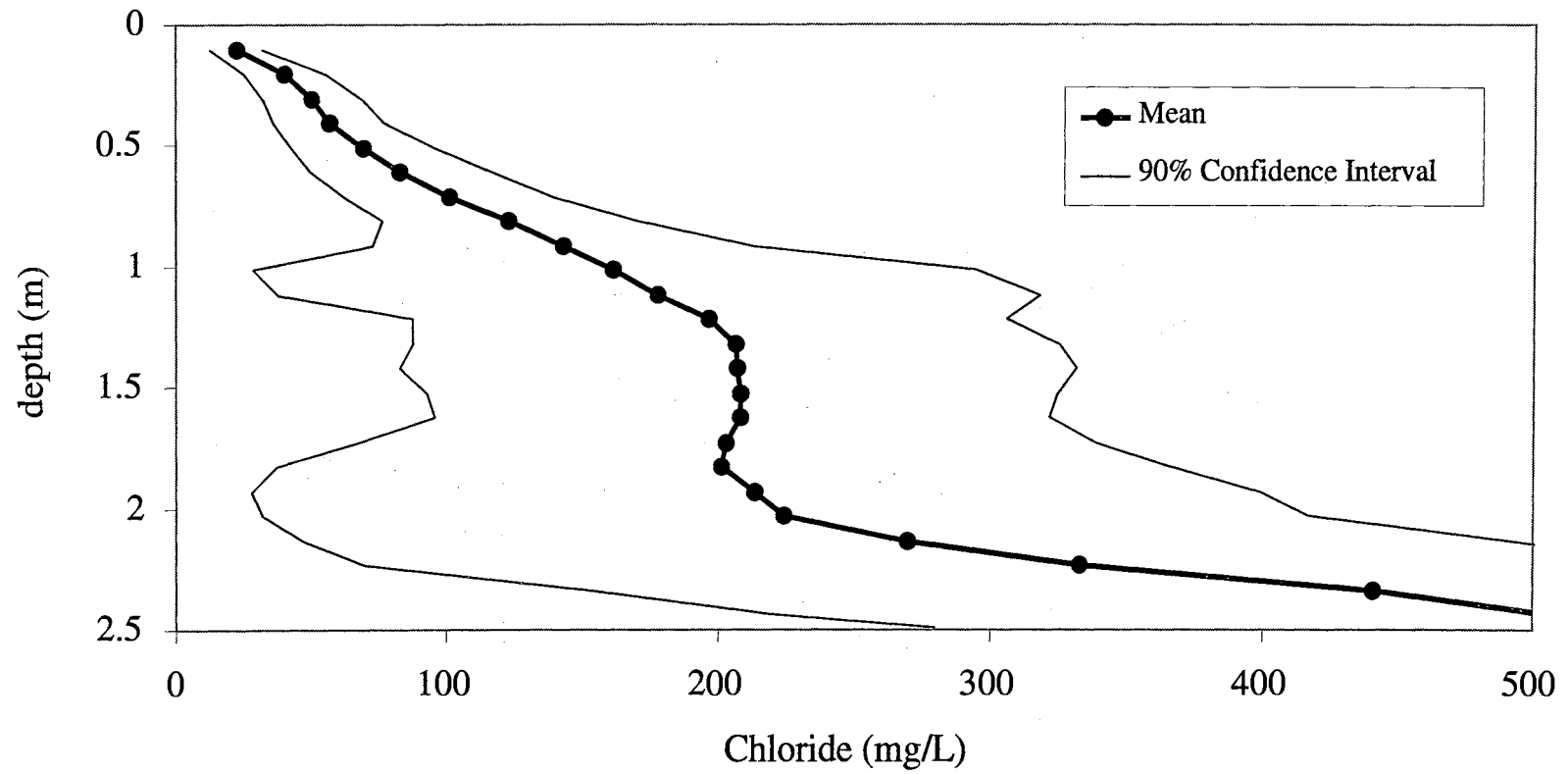
Figure 3-4. Sample mean and 90% confidence intervals of population mean for chloride concentrations of Group C cores.
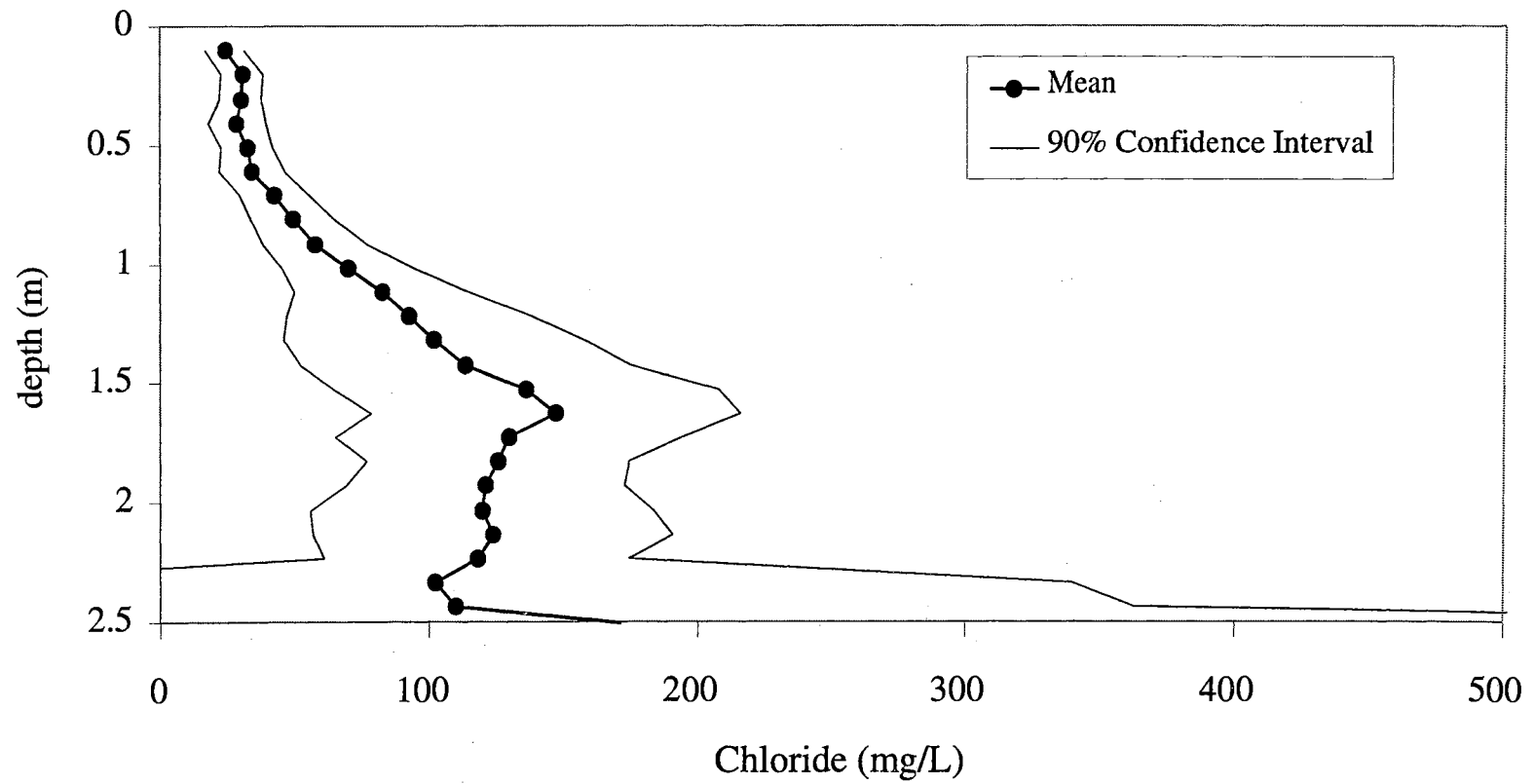
Figure 3-5. Sample mean and 90% confidence intervals of population mean for chloride concentrations of Group D cores.
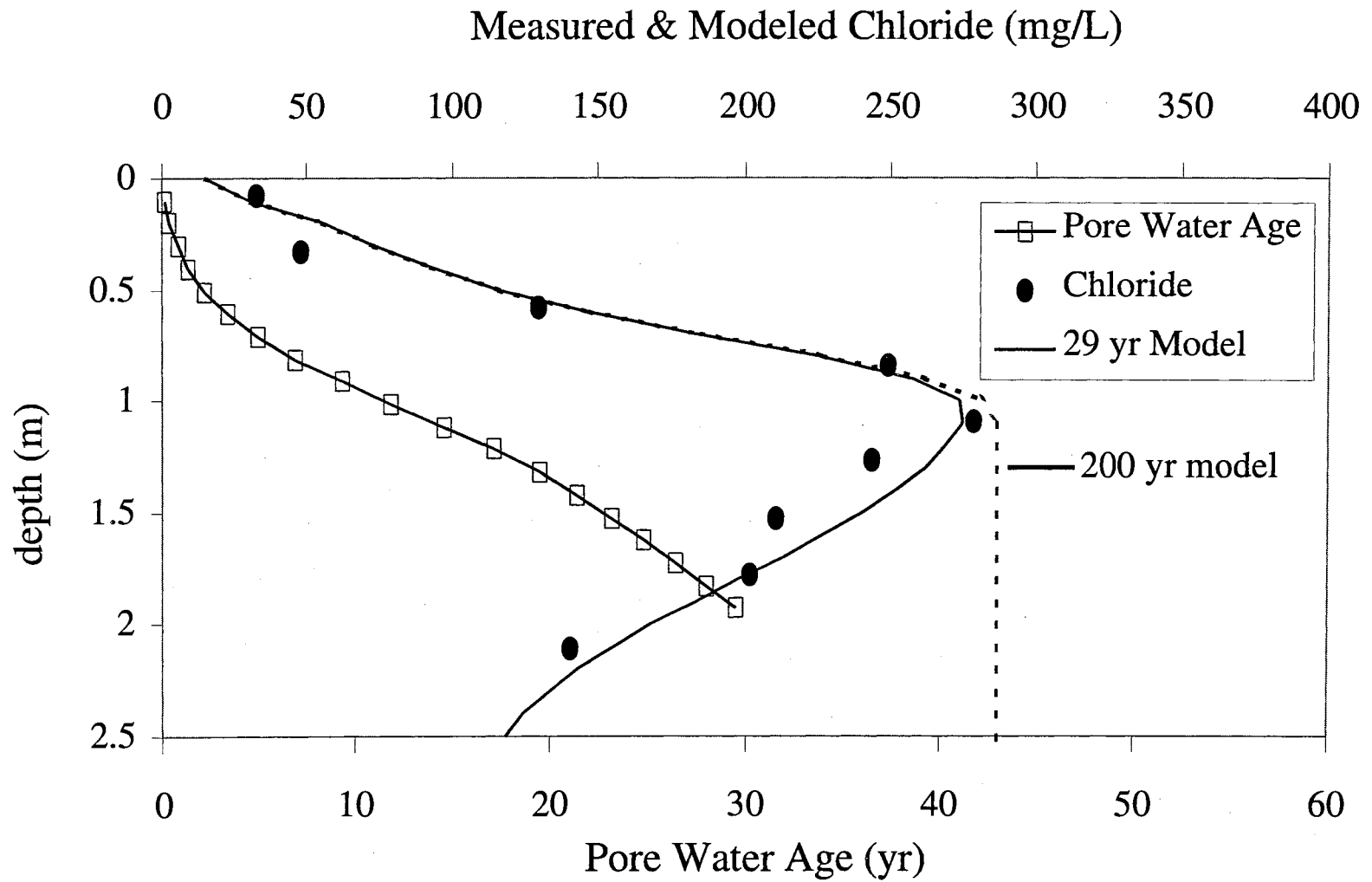
Figure 3-6. Modeling and pore water age of Core A-1-98.
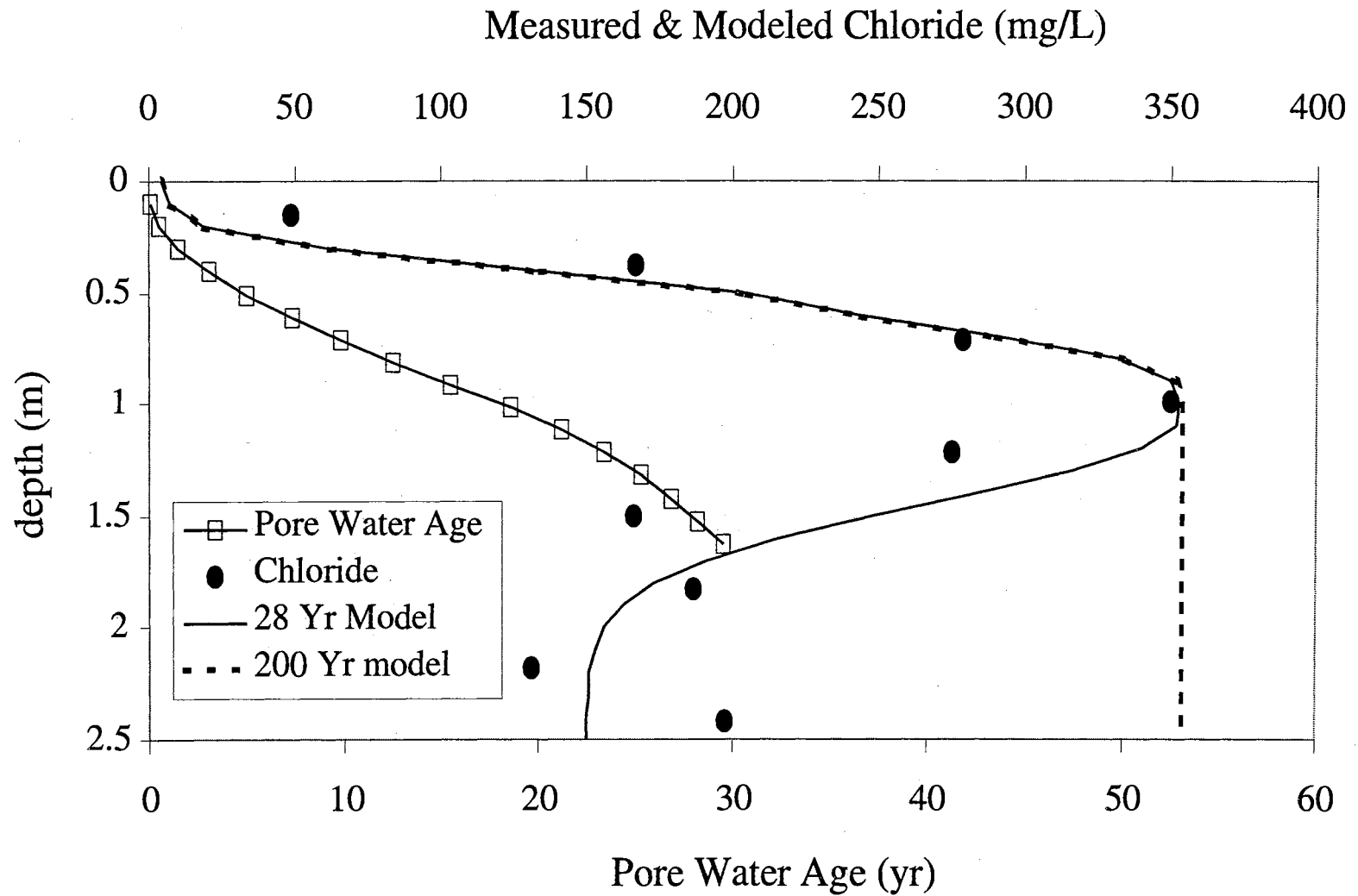
Figure 3-7. Modeling and pore water age of Core A-4-97.

CHAPTER IV

ESTIMATING A LONG TERM MONTHLY WATER BALANCE FOR KCl FERTILIZED WINTER WHEAT

4.1 Abstract

The objective of this research is to provide a historical interpretation of recharge, evapotranspiration, and runoff at a KCl fertilized field using deep continuous soil chloride profiles in conjunction with long-term meteorological data. Numerical modeling describes the relative magnitude of water flow into and out of the soil column. Although recharge, evapotranspiration, and runoff are all shown to be strongly related to precipitation, there does not appear to be a strong correlation between recharge and precipitation over time less than a few years.

4.2 Introduction

Estimating the inputs and outputs of water for agricultural plots is important for proper field management. Knowledge of precipitation, evapotranspiration, runon/runoff, and recharge enables informed decisions regarding plant variety, crop density, and timing of tillage and irrigation events. Even more important may be the prediction and mitigation of the consequences of climate variation. Although measuring precipitation is quite simple, direct measurement of evapotranspiration, runon/runoff, and recharge is difficult and rarely conducted; hence, they are often estimated from more easily measured

parameters. Of course, one of the water sources or sinks can be calculated using a water balance approach if the others are known.

Sixteen dryland winter wheat plots were initiated in 1969 at the Stillwater Agricultural Research Center. Fertilizer application has been consistent since 1969 and includes an annual application of KCl. The 34.4 $kgha^{-1}yr^{-1}$ of chloride applied as KCl acts as a tracer that is useful for interpreting the water balance. Additionally, the sixteen plots were separated into four groups of four plots with 0, 45, 90, or 134 $kg\, ha^{-1}\, yr^{-1}$ of N as NH_4NO_3. A previous study by Tyner et al. [2001] estimated the mean recharge rate of the plots using the Chloride Mass Balance Method assuming steady state conditions. They also provide a detailed description of the Chloride Mass Balance Method and plot management.

This study will attempt to model water and solute transport through the vadose zone for the 30 years the plots have existed using precipitation measurements, estimates of evapotranspiration and runoff, and Chloride Mass Balance. The estimates of evapotranspiration will be scaled to fit measured continuous soil core data assuming

$$R_e = P - E_t - Q \tag{4-1}$$

where R_e is recharge, P is precipitation, E_t is evapotranspiration, and Q is runoff. Runon is minimal since the plots are located on a local topographic high.

Three meter continuous soil cores were collected after the 1997 and 1998 growing seasons. Grain size, bulk density, moisture content, chloride concentration, and nitrate concentration were measured at approximately 0.3 m depth intervals. Details of the sampling and laboratory techniques are available in Tyner et al. [2001]. In contrast to the Chloride Mass Balance Method, steady state conditions were not assumed for this study.

A non-steady condition allows for the optimization of water balance inputs over time; therefore allowing inferences to be made between measured P and estimates of R_e, E_t, and Q, which might allow for improved management of agricultural assets.

4.3 Initial Estimate of E_t

A common approach for estimating E_t, involves first estimating evapotranspiration for a reference crop (E_{to}) such as grass or alfalfa (referred to as reference crop evapotranspiration or potential evapotranspiration). E_{to} can be measured directly or estimated by a number of methods. E_t is then calculated by multiplying E_{to} by a crop coefficient, K_c, which is an experimentally defined crop-specific parameter whose value varies throughout the growing season.

$$E_t = K_c E_{to} \qquad (4\text{-}2)$$

This study initially estimates E_{to} using the method of *Hargreaves et al.*, [1985], a method based solely on temperature and latitude, and represented by

$$E_{to} = 0.0023 R_A \ TD^{\frac{1}{2}}(T+17.8) \qquad (4\text{-}3)$$

where TD is difference of the mean monthly maximum and minimum temperatures; T is the mean monthly temperature; and R_A is extraterrestrial radiation. *Duffie and Beckman*, [1980] represent R_A by

$$R_A = (24(60)/\pi)G_{SC} \ d_r[(\omega_s)\sin(\phi)\sin(\delta)+\cos(\phi)\sin(\delta)\sin(\varpi_s)] \qquad (4\text{-}4)$$

where

$$\delta = 0.4093\sin(2\pi \ (284+J)/365)$$

$$d_r = 1+0.033\cos(2\pi \ J/365)$$

$$\omega_s = \arccos\left(-\tan(\phi)\tan(\delta)\right).$$

and G_{SC} is the solar constant with a value of $0.0820 \text{ MJ m}^{-2}\text{min}^{-1}$.

The values for K_c of winter wheat are estimated from data within *Howell et al.*, [1995]. Although the values from *Howell et al.* [1995] represent sprinkler irrigated winter wheat, only the relative shape of K_c versus time is of importance, not the magnitude of the values, since E_t calculated from (4-2) will be further scaled to render a proper chloride distribution with depth. Observations of winter wheat K_c distributions from other studies are similar in shape [*Hunsaker, et al.*, 2000; *Tyagi, et al.*, 2000].

4.4 Initial Estimates of Runoff

A common method to estimate Q is to apply the *Soil Conservation Service's* [1985] runoff equation

$$Q = \frac{(P - 0.2S)^2}{P + 0.8S}; \qquad P \geq 0.2S \tag{4-3}$$

with

$$S = \frac{1000}{CN} - 10 \tag{4-4}$$

where CN is the curve number and is a function of field management and soil type. The Kirkland clay loam soil (fine, mixed, thermic Udertic Paleutoll) in which the plots are located is defined as hydrologic group D. The predicted CN for the plots ranges from 84 to 88 [*Soil Conservation Service*, 1985]. Daily measured precipitation data was used for an initial estimate of daily Q using (4-3) and (4-4). Daily values of Q were summed to provide monthly values of Q.

4.5 Modeling

4.51 Hydrus 1-D

Numerical modeling was conducted using Hydrus 1-D version 7.0 [1998] to enable scaling of individual components of (4-1), while retaining the variability of monthly values. The numerical model was used to solve the Richards equation for one-dimensional transport of water and chloride in variably saturated media while including a sink term to account for water uptake by plant roots. An initial model time step of 0.1 days with a maximum of 1 day was used for a duration of 28.9 years, the duration of the winter wheat plots prior to soil core collection. The van Genuchten parameters describing soil hydraulic properties were initially estimated based on grain size analysis and were further refined by matching modeled and measured soil water contents. Since the soil hydraulic properties are very strong functions of water content, errors describing van Genuchten properties in a system with assumed known water inputs manifests itself by small errors in the modeled water content until proper amounts of water transmission can occur.

4.52 Boundary Conditions

A variable upper boundary determined from equilibrium conditions between soil water and atmospheric water vapor was applied with the potential for ponding of water to occur at the surface. Indistinguishable results were obtained using an upper boundary condition without ponding potential, since ponding did not occur during the simulation. The fact that ponding or runoff did not occur in the model would be problematic except

67

for the fact that all inputs including precipitation were represented by monthly values, thereby reducing the magnitude of precipitation from individual events. Entering precipitation at the measured daily intervals might produce more precise results, but would still moderate precipitation intensity to a significant degree.

The upper chloride concentration was modeled as a constant concentration equaling the net annual chloride applied to the plots divided by the sum of precipitation minus the sum of runoff. This is an acceptable simplification due to the low transport rates of water and solutes within the fine textured soil. The lower boundary condition was modeled as a zero hydraulic gradient and constant chloride concentration flux at a depth adequate to preclude a significant influence on the simulation. An initial chloride concentration distribution was chosen to have a constant concentration from the root depth to the base of the model that was similar to the measured chloride concentration at the base of the soil cores. A linear chloride concentration gradient was used between the surface and the root depth.

4.53 Model Inputs

The monthly inputs into the model included potential evaporation, potential transpiration, and the net precipitation, P_{net}, calculated by subtracting Q from P. Potential evaporation was set to zero and the potential transpiration input corresponded to the linearly scaled version of E_t calculated in section 4.3. The distribution of potential transpiration versus depth within the model was optimized such that the measured and modeled chloride concentration distributions versus depth were similar. By doing so,

evaporation was effectively represented in the model by transpiration from the soil surface, which is equivalent to evaporation.

The initial estimate of E_t was linearly scaled by a coefficient since the model requires potential evapotranspiration, not E_t. By using potential evapotranspiration, the model avoids removal of water from nodes in a manner inconsistent from reality, such as delivering water through the soil profile at a rate beyond that predicted by soil hydraulic properties. Using a linearly scaled version of E_t instead of the E_{to} calculated from (4-3) allows for seasonal variation specific to winter wheat evapotranspiration to be included in the model. The magnitude of the coefficient was optimized to enable matching of the modeled and measured chloride concentration distributions. A weakness of entering a linearly scaled version of E_t as potential transpiration into the model is that seasonal variation in K_c due to the distribution of P seasonally is effectively doubled. An alternative of entering E_{to} calculated from (4-3) as potential transpiration was not chosen due to the complete loss of the prominent E_t seasonal variation associated with the winter wheat life cycle.

4.54 Chloride Mass Balance

Since plants do not take up significant amounts of chloride, the process of evapotranspiration causes an increase in the chloride concentration as water moves downward through the soil column. Beneath the root zone no additional water is removed and chloride concentrations are constant with depth if long-term steady state conditions are assumed. By increasing or decreasing the E_t coefficient, the chloride

concentrations in the root zone can be manipulated to higher and lower concentrations, respectively.

4.55 Runoff versus Evapotranspiration

Initial attempts to model the plots without Q failed to match the measured chloride distribution. During dry periods an appropriate chloride distribution would begin to grow in the root zone, but then during periods of high precipitation, the entire chloride profile would move downward beneath the root zone followed by construction of a subsequent chloride bulge in the root zone. Applying (4-3) to reduce P to P_{net} reduced the tendency of very wet periods to drive the chloride concentrations beneath the measured locations.

Balancing the relative amounts of water loss between E_t and Q is problematic since the vast majority of chloride applied to the plots occurred during a single fertilization event each fall. If Q occurs during summer months, water is lost from the plots, but the chloride mass lost is insignificant due to the relatively low chloride concentration in precipitation; therefore, regarding a mass balance of chloride in and out of the plots, Q is almost indistinguishable from evaporation as they both remove water from the surface without significant removal of chloride mass. The only difference is the way in which the removal of water manifests itself. An increase of water removal by Q is primarily from the large precipitation, which is in contrast to the more evenly distributed water loss as produced by an increase of E_t. Therefore increasing Q leads to a chloride concentration distribution that is smoother with less small-scale variability over depth. A lower limit for Q can be identified such that the chloride profiles are not driven beneath

the root zone during wet periods. With the exception of P, a reasonable upper limit for Q is not apparent.

4.6 Results

Two cores were modeled using inputs described previously, while maintaining proper chloride concentration and water distributions. The first core had no N added annually and was initially modeled with a curve number of 84, which led to 5.3 m of runoff over the 28.9 years modeled using (4-3). Optimization of E_t scaling and the relative amounts of E_t per depth was accomplished such that the measured and modeled chloride concentrations are similar after the 28.9 year model run as shown in figure 4-1. At 9.5 years a chloride pulse begins to build at approximately 0.85 m, but between 9.5 and 19.1 years above average precipitation moves the chloride pulse to approximately 1.2 m, which is below the modeled and measured root depth of 1.0 m. Between 19.1 and 28.6 years, more moderate precipitation occurs and the chloride pulse resides at approximately 1.0 m, although remnants of the chloride pulse at 19.1 years are still apparent.

To demonstrate the lack of model sensitivity for water loss from Q versus E_t, a second modeling effort of the same soil core was completed using a curve number of 88, which led to 7.2 m of runoff. All other parameters were identical except for E_t, which was linearly scaled down to compensate for increased Q. The modeling predicts very similar chloride concentration distributions as shown in figure 4-2. The maximum concentration of the chloride pulses is slightly greater at 9.5 and 19.1 years and slightly

less at 28.6 years. A continuously applied tracer would be beneficial towards determining the relative ratio between P and E_t.

Figure 4-3 shows the predictions of surface infiltration, P, Q, and E_t for the model with a curve number of 88. As expected, all of the distributions are strongly related. Q acts as a buffer to surface infiltration since it only occurs during large P events. Figure 4-4 demonstrates the amount of buffering by displaying the difference of P, Q, and $(P-Q)$ from their respective means. This buffering is what inhibits the chloride pulses from being driven beneath the root zone during wet periods.

Many years the net surface flux is negative, as indicated by E_t being greater than the surface infiltration in figure 4-3. Figure 4-5 demonstrates this more clearly by relating $P - Q - E_t$ to $P - Q$. The two distributions do not always appear to be strongly related, which is caused by the very long residence time of water in the root zone. Since many years go by before water passes beneath the root zone, a given control volume of water experiences many relatively wet and dry periods, and because much of the E_t takes place at a depth that is somewhat insulated from the surface, the relative amount of E_t is more a function of growth stage, temperature, and relative pore water availability than current precipitation rates. Put more simply, the roots at 0.5 m are extracting water as a function of growth stage and pore water available rather than current weather conditions. Roots beneath the near surface are therefore partially insulated from current P.

The second core had 134 kg ha^{-1} yr^{-1} of N added as NH_4NO_3 and was modeled with a curve number of 88. Results of modeling are plotted in figure 4-6. The initial chloride distribution is identical to the no N core and has a concentration of 150 mg/L beneath the root zone, as this was common among the soil cores collected. Using

reasonable values for E_t and root density distribution, the chloride pulse at 1.5 m could not be reproduced. It is possible that if the curve number was varied as a function of time to account for differing surface conditions over the winter wheat life cycle, a better fit could be rendered. Another possibility is to modify the root density over time such that the depth E_t occurs is also a function of the winter wheat life cycle.

Figure 4-7 displays the surface infiltration, P, Q, and E_t as a function of time and shows an almost constant net downward flux at the surface. This is more clearly seen in figure 4-8, which displays surface infiltration minus E_t versus the difference from the mean of P minus Q. The net surface flux matches the distribution of P minus Q slightly better than in the first core, although still minimally, which would be expected since a higher recharge rate limits the insulation of the lower root zone from current P by upper soils. Indeed, although quite varied, the net surface flux is positive downward throughout almost the entire simulation. It seems that short term prediction of net surface flux based on knowledge of current P is a difficult undertaking

4.7 Conclusions

Development and calibration of a hydrological model to estimate infiltration, E_t, and Q using knowledge of temperature, P, and chloride concentration distributions is possible, but difficult. The model developed for this study demonstrates the buffering capacity that Q has on infiltration and shows the somewhat random nature of the relationship between annual P and net surface flux, which is due to the lack of hydraulic connectivity between the lower root zone and the surface. Insulation of the lower root zone is more apparent in soil cores with a lower recharge rate. A lower recharge rate

implies an older age of water at any given depth, and therefore more time is represented between deep soil water and surface conditions.

The modeling does reflect the relative magnitudes of the different sources and sinks of water for dryland winter wheat production near Stillwater, Oklahoma and such a model has potential to describe the impact that long-term changes of climate might have on regional grain production. Improvements to the model include varying root density and curve number over time to more accurately represent the winter wheat growth cycle. Additionally, more confidence in either the predicted Q or E_t would allow for more accurate calculation of the E_t or Q, respectively. Finally, field scale variability as demonstrated by the two modeled cores is sufficient to require that numerous locations within a small area be modeled for results to be more meaningful.

4.8 References

Duffie, J. A., and W. A. Beckman, *Solar Engineering of Thermal Processes*. John Wiley and Sons, New York., 1-109, 1980.

Hargreaves, G. H. and Z. A. Samani, Reference crop evapotranspiration from temperature. *Applied Engrg. In Agric.*, 1:96-99, 1985.

Howell, T. A., J. L. Steiner, A. D. Schneider, S. R. Evett, Evapotranspiration of irrigated winter wheat — southern high plains. *Transactions of the ASAE*, 38:745-749, 1995.

Hunsaker, D. J., B. A. Kimball, P. J. Pinter Jr., G. W. Wall, R. L. LaMorte, F. J. Adamsen, S. W. Leavitt, T. L. Thompson, A. D. Matthias, T. J. Brooks, CO_2 enrichment and soil nitrogen effects on wheat evapotranspiration and water use efficiency. *Agric. For. Meteorol.*, 104:85-105, 2000.

Hydrus, Golden CO.: International Ground Water Modeling Center. Software Package for Simulating the One-Dimensional Movement of Water, Heat and Multiple Solutes in Variably Saturated-Media Ver. 2.0, pp. 1-178. Golden CO.: Colorado School of Mines, 1998.

Soil Conservation Service, Hydrology. Section 4, Soil Conservation Service National Engineering Handbook. U.S. Department of Agriculture, Washington D.C., 1985.

Tyagi, N. K., D. K. Sharma, S. K. Luthra, Evapotranspiration and crop coefficients of wheat and sorghum. *J. Irrig. And Drain. Div*, 126:215-222,2000.

Tyner, J. S., G. O. Brown, J. R. Vogel, J. Garbrecht, Chloride mass balance to determine water fluxes beneath KCl fertilized crops. *Transactions of the ASAE*, 43:1553-1559, 2001.
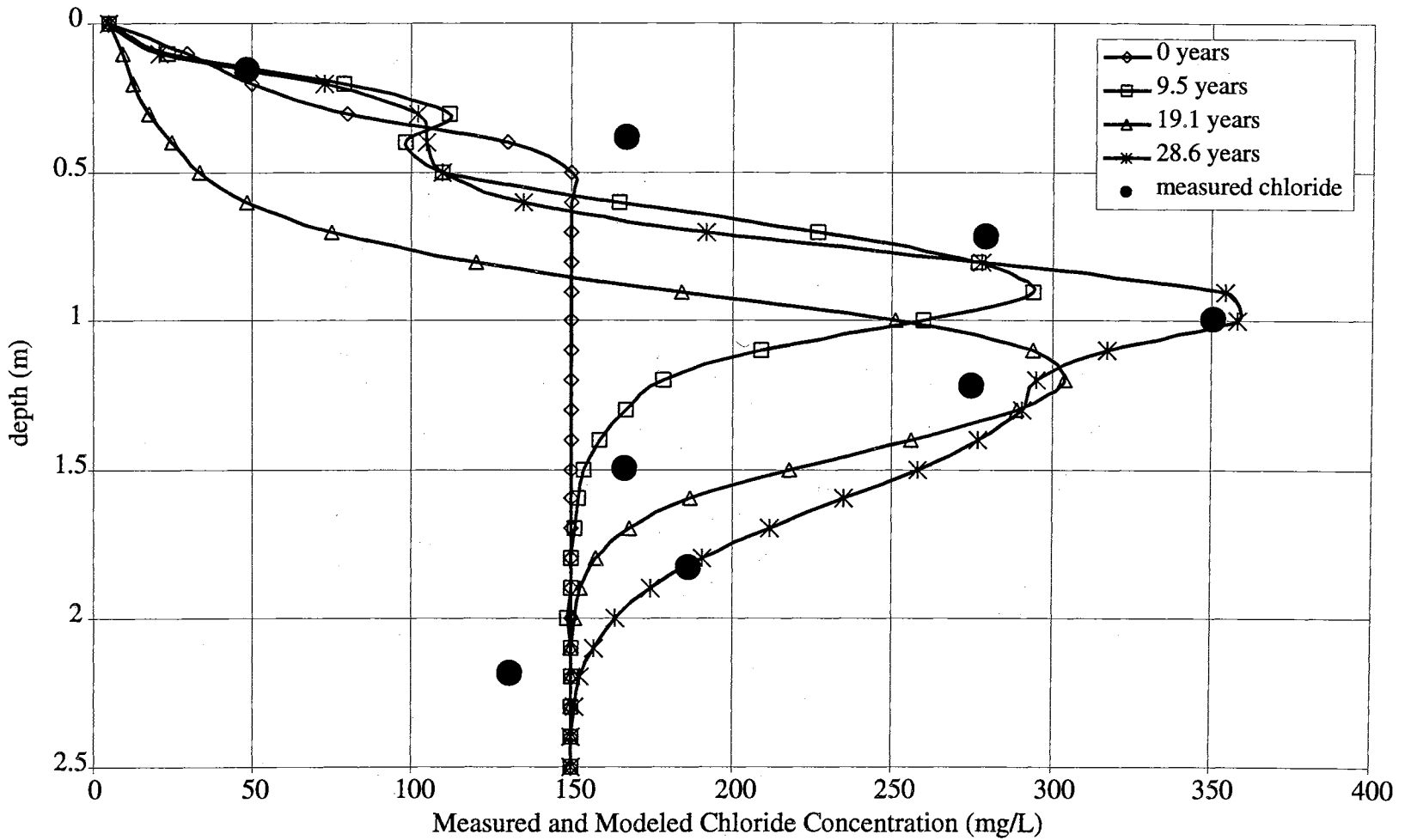
Figure 4-1. Modeling of 0 N core with a curve number of 84.
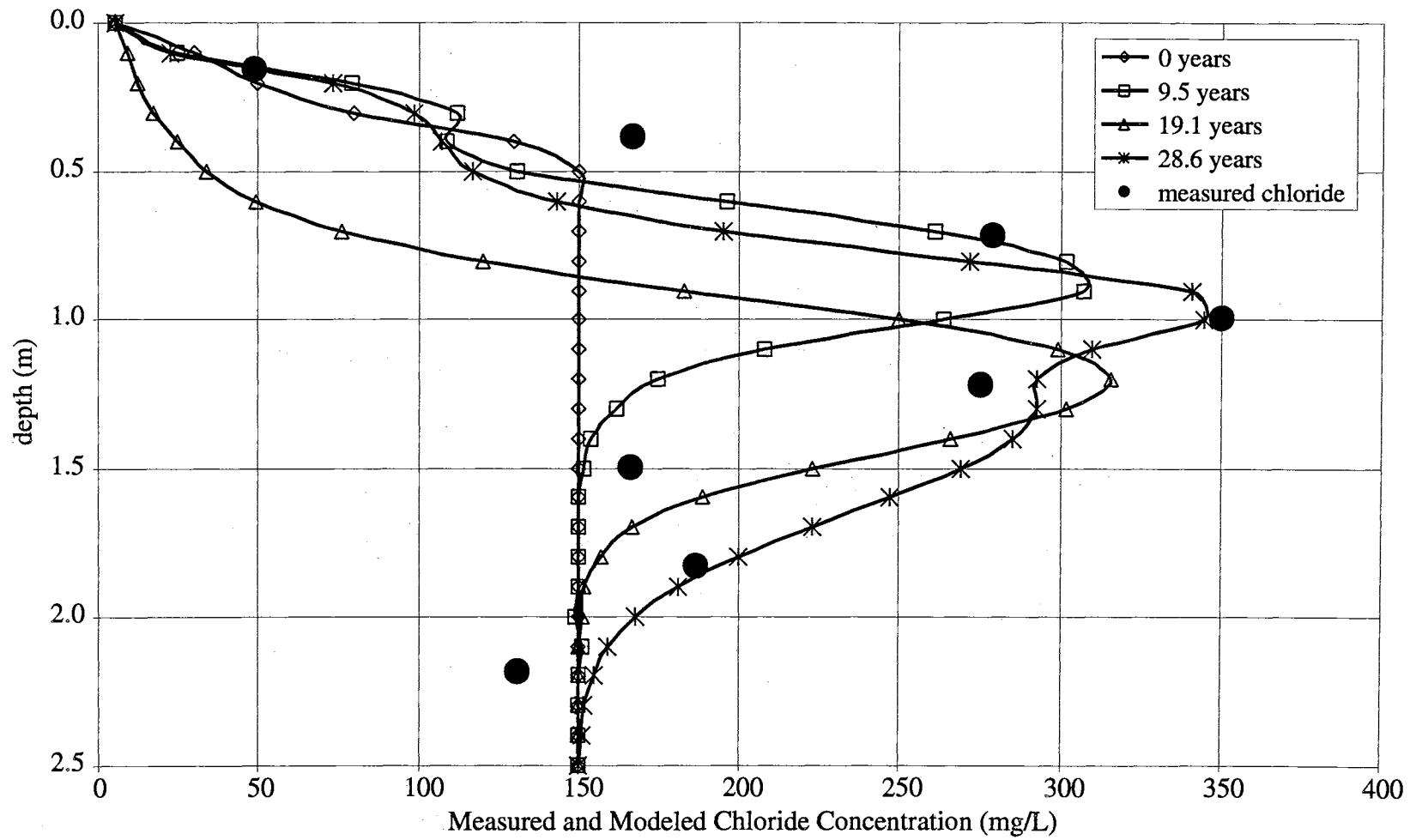
Figure 4-2. Modeling of 0 N core with a curve number of 88.
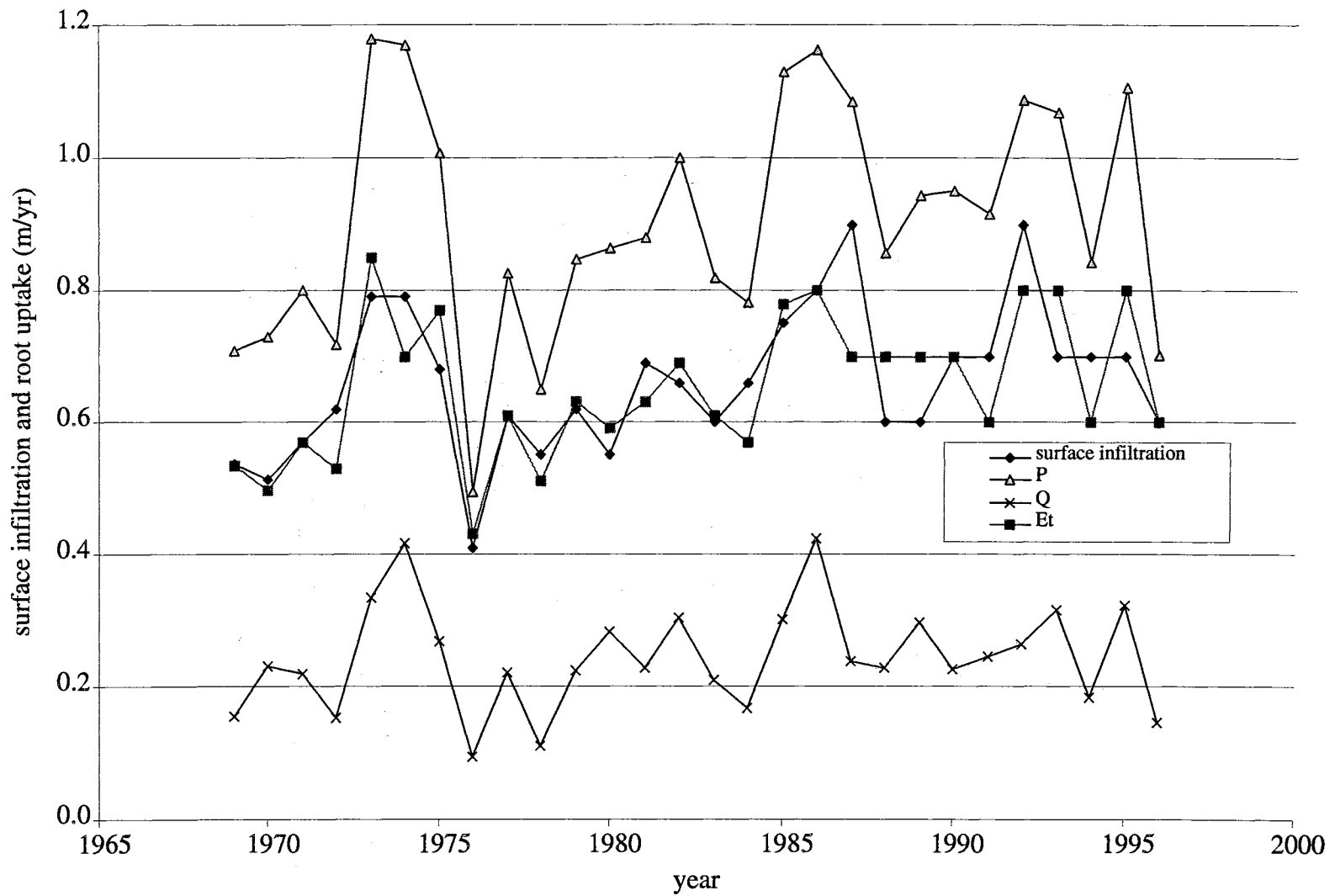
Figure 4-3. Comparison of surface infiltration, P, Q, and E_t of 0 N core.
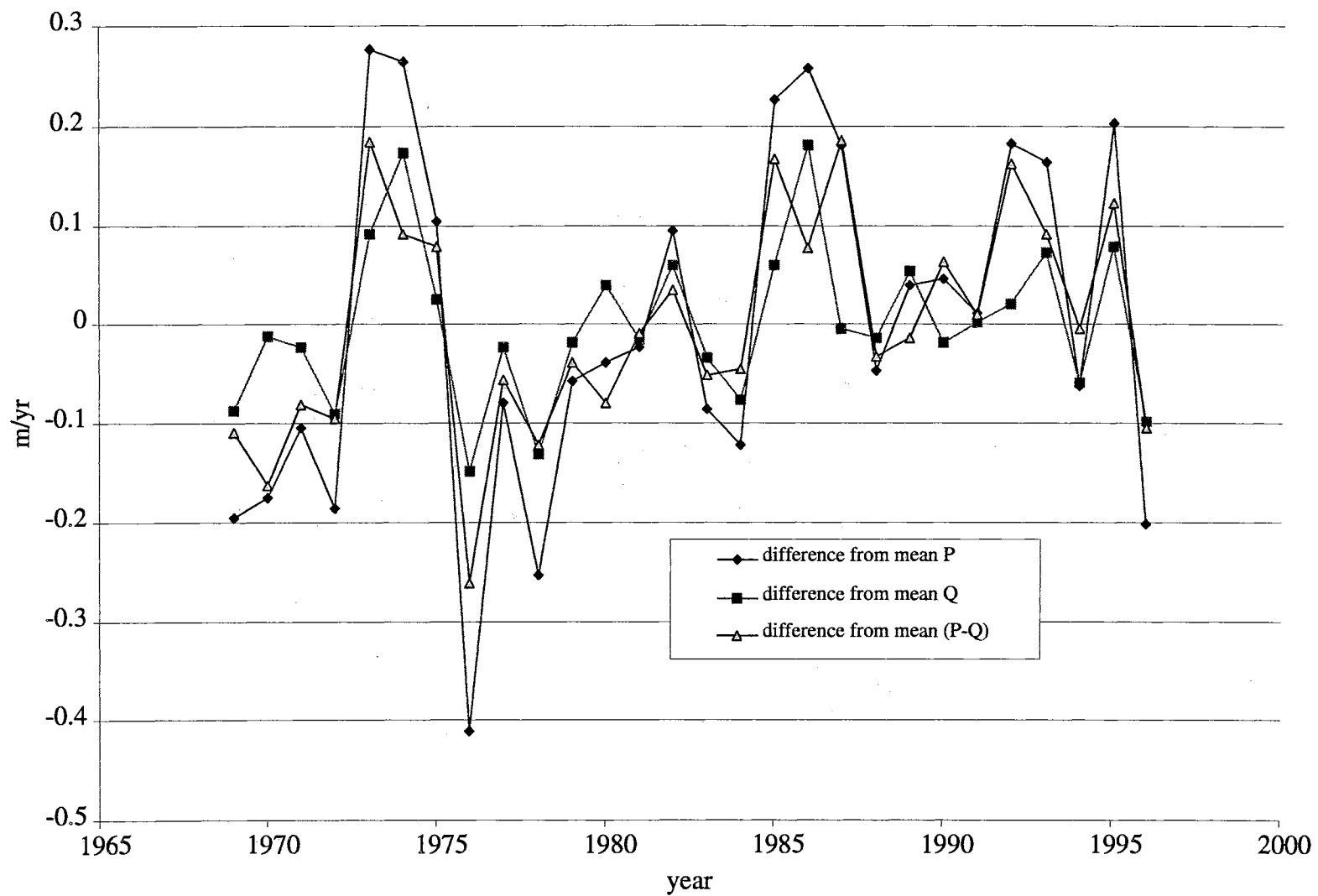
Figure 4-4. Comparison of the difference from mean *P*, *Q*, and (*P-Q*) of 0 N core.
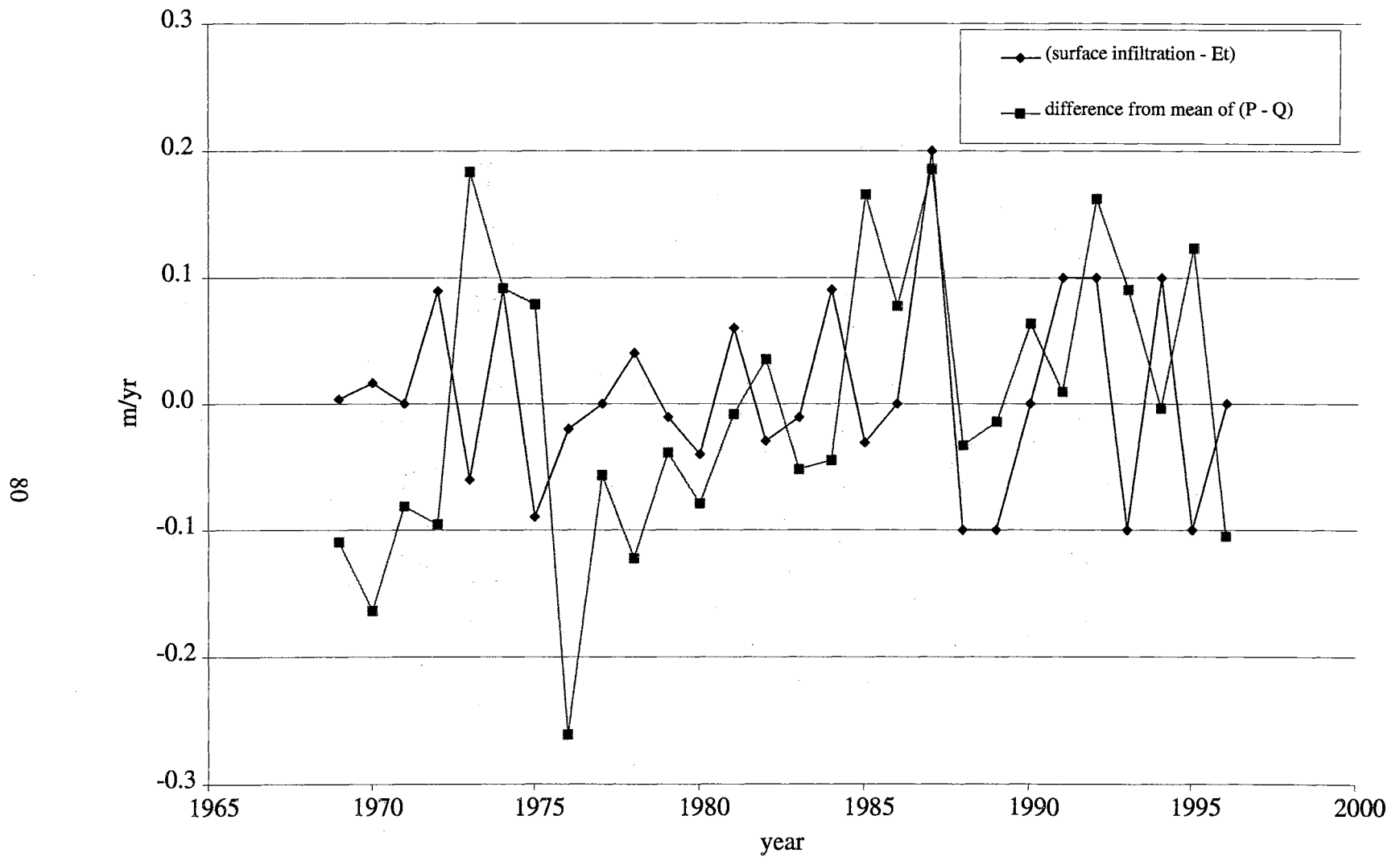
Figure 4-5. Comparison of (surface infiltration - E_t) and difference from the mean of (P-Q) of 0 N core.
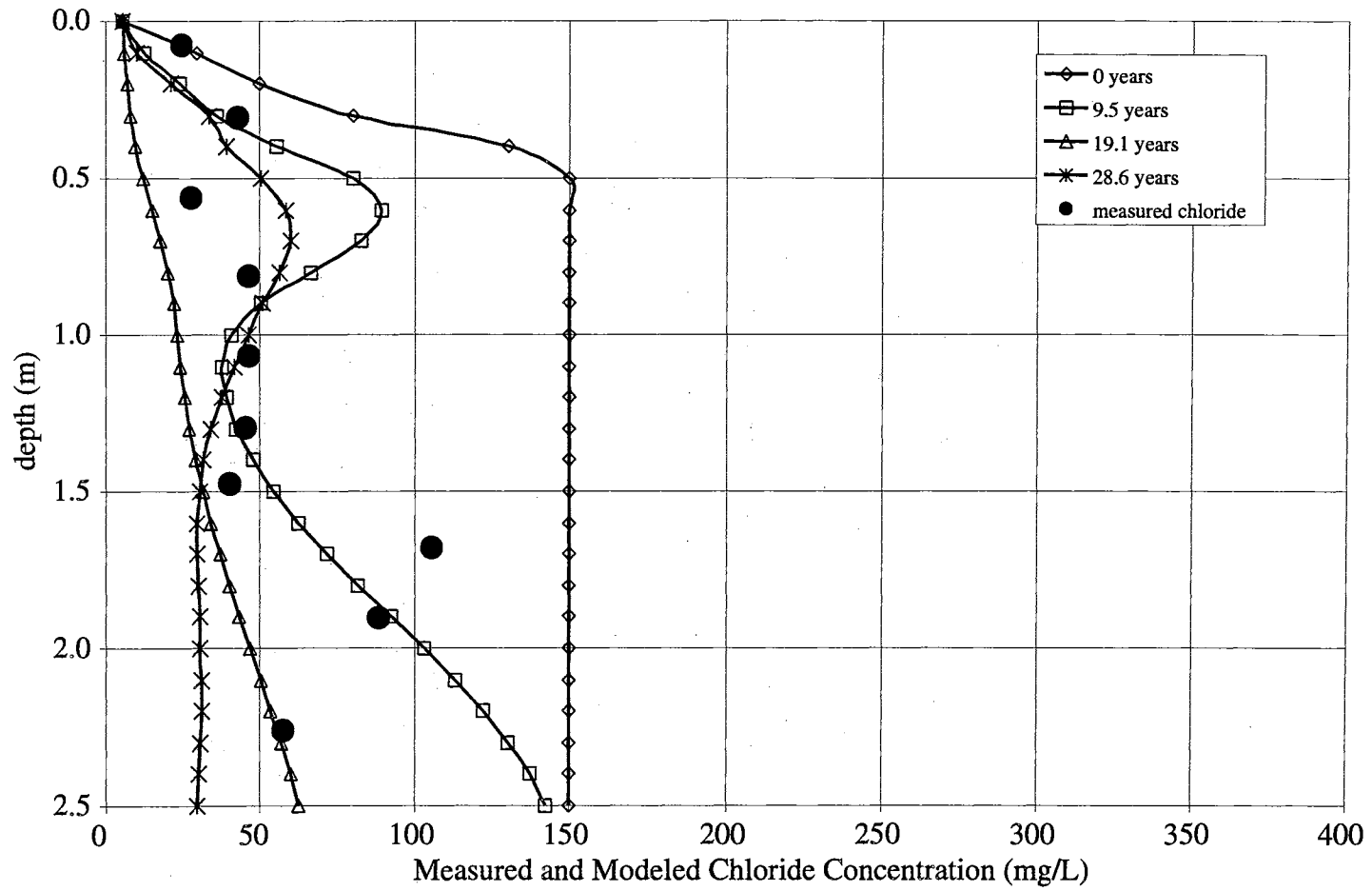
Figure 4-6. Modeling of 134 kg ha^{-1} yr^{-1} N core with a curve number of 88.
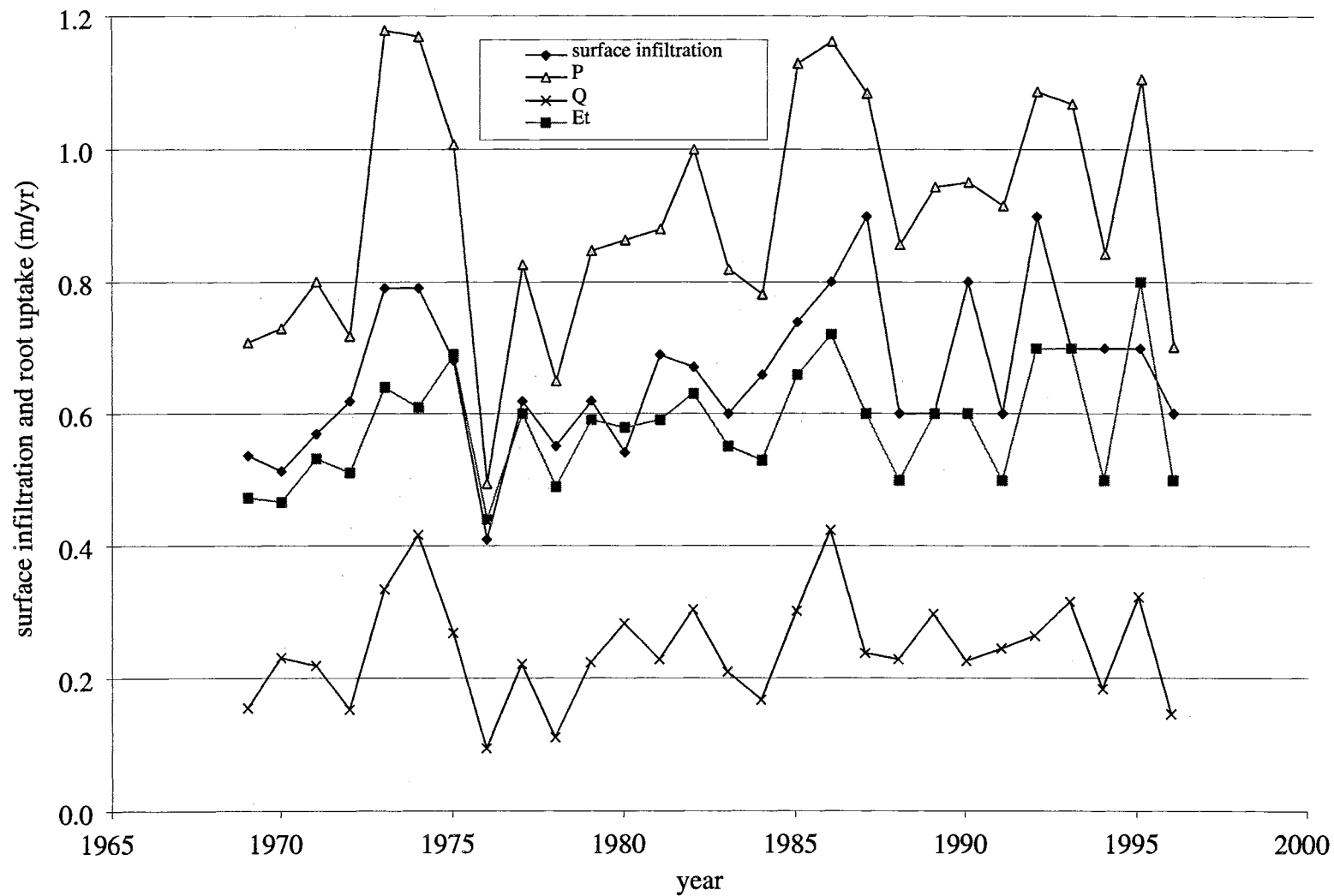
Figure 4-7. Comparison of surface infiltration, P, Q, and E_t of 134 kg ha^{-1} yr^{-1} N core.
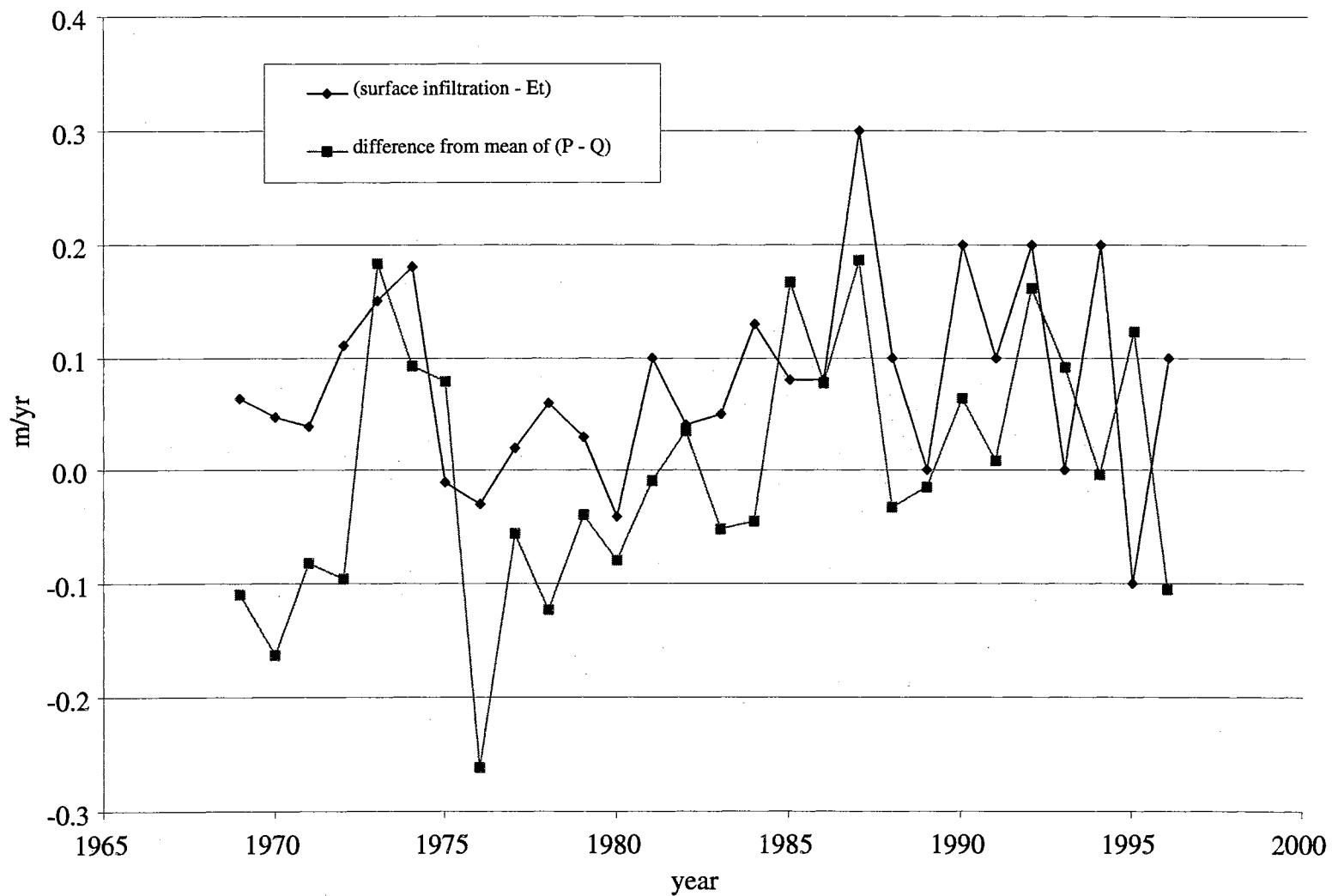
Figure 4-8. Comparison of (surface infiltration - E_t) and difference from the mean of (P-Q) of 134 kg ha^{-1} yr^{-1} N core.

APPENDICES

Appendix A Data from Slaughterville Sandy Loam Bruce-Klute Test

Table A-1. Data from Slaughterville Sandy Loam Bruce-Klute Test

Distance from Inlet (mm)	θ	λ (mm/s$^{-1/2}$)
100	12.0	28.831
100	70.7	11.894
100	129.3	8.793
100	188.0	7.294
100	246.6	6.368
100	305.3	5.723
100	363.9	5.242
100	422.6	4.864
100	481.2	4.559
100	539.8	4.304
100	598.4	4.088
100	657.0	3.901
100	715.4	3.739
100	773.7	3.595
100	832.1	3.467
100	890.5	3.351
100	948.8	3.247
100	1006.9	3.151
100	1064.9	3.064
100	1122.9	2.984
100	1180.7	2.910
100	1238.3	2.842
100	1295.8	2.778
100	1353.3	2.718
100	1410.7	2.662
100	1468.1	2.610
100	1525.5	2.560
100	1582.8	2.514
100	1640.2	2.469
100	1697.5	2.427
100	1754.8	2.387
100	1812.1	2.349
100	1869.3	2.313
100	1926.6	2.278
100	1983.8	2.245
100	2041.0	2.213
100	2098.3	2.183
100	2155.5	2.154
100	2212.7	2.126
100	2269.9	2.099
100	2327.1	2.073
100	2384.3	2.048
100	2441.5	2.024

Distance from Inlet (mm)	θ	λ (mm/s$^{-1/2}$)
100	2498.6	2.001
100	2555.8	1.978
100	2613.0	1.956
100	2670.1	1.935
100	2727.3	1.915
100	2784.5	1.895
100	2784.5	1.895
100	2841.6	1.876
100	2898.8	1.857
100	2955.9	1.839
100	3013.0	1.822
100	3070.2	1.805
100	3127.3	1.788
100	3184.4	1.772
100	3241.6	1.756
100	3298.7	1.741
110	41.5	17.071
110	100.2	10.991
110	158.8	8.728
110	217.5	7.459
110	276.1	6.620
110	334.8	6.012
110	393.4	5.546
110	452.1	5.174
110	510.7	4.868
110	569.3	4.610
110	627.9	4.390
110	686.4	4.199
110	744.7	4.031
110	803.1	3.882
110	861.5	3.748
110	919.8	3.627
110	978.1	3.518
110	1036.1	3.418
110	1094.1	3.326
110	1152.0	3.241
110	1209.7	3.163
110	1267.2	3.090
110	1324.8	3.022
110	1382.2	2.959
110	1439.6	2.899
110	1497.0	2.843
110	1554.3	2.790
110	1611.7	2.740
110	1669.0	2.693

Distance from Inlet (mm)	θ	λ (mm/s$^{-1/2}$)
110	1726.3	2.648
110	1783.6	2.605
110	1840.9	2.564
110	1898.1	2.525
110	1955.4	2.488
110	2012.6	2.452
110	2069.8	2.418
110	2127.1	2.385
110	2184.3	2.354
110	2241.5	2.324
110	2298.7	2.294
110	2355.9	2.266
110	2413.1	2.239
110	2470.2	2.213
110	2527.4	2.188
110	2584.6	2.164
110	2641.7	2.140
110	2698.9	2.118
110	2756.0	2.095
110	2813.2	2.074
110	2870.4	2.053
110	2927.5	2.033
110	2984.7	2.014
110	3041.8	1.995
110	3098.9	1.976
110	3156.1	1.958
110	3213.2	1.941
110	3270.3	1.924

Appendix B Data from the Agricultural Experiment Station Soil Samples

Table B-2. Data from the Agricultural Experiment Station Soil Samples

Year	Group	Repetition	Depth (m)	θ	Cl^{-1} (mg/L)	NO_3-N(mg/L)
1997	A	1	0.08	0.12	84.0	13.6
1997	A	1	0.33	0.23	99.4	0.0
1997	A	1	0.53	0.18	171.2	5.4
1997	A	1	0.81	0.16	228.3	0.0
1997	A	1	0.97	0.16	144.5	0.0
1997	A	1	1.32	0.18	61.0	0.0
1997	A	1	1.52	0.14	210.8	0.0
1997	A	1	1.80	0.15	253.4	5.8
1997	A	1	2.01	0.14	199.5	5.5
1997	A	1	2.16	0.15	230.2	0.0
1997	A	1	2.39	0.15	199.7	7.9
1997	A	1	2.64	0.15	101.5	0.0
1997	A	2	0.08	0.11	58.8	2.6
1997	A	2	0.25	0.21	134.7	0.0
1997	A	2	0.43	0.15	178.7	0.0
1997	A	2	0.64	0.14	335.6	0.0
1997	A	2	0.86	0.15	212.5	0.0
1997	A	2	1.02	0.16	295.9	0.0
1997	A	2	1.27	0.17	397.0	0.0
1997	A	2	1.47	0.16	237.2	0.0
1997	A	2	1.65	0.17	168.6	0.0
1997	A	2	1.91	0.15	63.5	0.0
1997	A	2	2.16	0.15	135.5	0.0
1997	A	2	2.49	0.17	337.3	6.2
1997	A	3	0.10	0.15	17.1	5.1
1997	A	3	0.25	0.23	50.5	0.0
1997	A	3	0.61	0.16	190.2	0.0
1997	A	3	0.81	0.16	324.9	0.0
1997	A	3	1.07	0.17	287.4	0.0
1997	A	3	1.22	0.20	223.6	0.0
1997	A	3	1.45	0.18	195.4	0.0
1997	A	3	1.63	0.16	203.3	6.9
1997	A	3	1.85	0.14	167.2	17.6
1997	A	3	2.06	0.13	222.0	25.5
1997	A	3	2.21	0.13	219.7	33.1
1997	A	3	2.49	0.14	216.4	35.6
1997	A	4	0.15	0.18	48.7	0.0
1997	A	4	0.38	0.21	167.0	0.0
1997	A	4	0.71	0.19	279.1	0.0
1997	A	4	0.99	0.18	350.1	0.0
1997	A	4	1.22	0.15	275.0	0.0
1997	A	4	1.50	0.15	166.4	0.0

Year	Group	Repetition	Depth (m)	θ	Cl^{-1} (mg/L)	NO_3-N(mg/L)
1997	A	4	1.83	0.17	186.3	0.0
1997	A	4	2.18	0.17	130.9	8.2
1997	A	4	2.41	0.18	197.3	15.0
1997	B	1	0.10	0.15	24.1	7.4
1997	B	1	0.38	0.20	31.8	0.9
1997	B	1	0.53	0.17	48.5	0.0
1997	B	1	0.79	0.15	54.6	5.9
1997	B	1	1.04	0.17	87.4	0.0
1997	B	1	1.27	0.19	182.1	0.0
1997	B	1	1.47	0.16	48.6	0.0
1997	B	1	1.70	0.15	49.5	0.0
1997	B	1	1.91	0.13	71.5	0.0
1997	B	1	2.08	0.13	65.8	0.0
1997	B	1	2.36	0.15	80.5	0.0
1997	B	1	2.62	0.17	219.9	21.3
1997	B	2	0.05	0.11	51.7	52.9
1997	B	2	0.28	0.21	136.4	7.6
1997	B	2	0.51	0.21	292.3	0.9
1997	B	2	0.69	0.17	277.9	0.5
1997	B	2	0.99	0.18	318.3	0.0
1997	B	2	1.24	0.18	289.8	0.0
1997	B	2	1.50	0.18	386.4	0.0
1997	B	2	1.75	0.17	312.4	4.8
1997	B	2	1.98	0.17	393.3	8.0
1997	B	2	2.24	0.17	434.5	8.4
1997	B	3	0.08	0.13	74.7	22.7
1997	B	3	0.28	0.24	71.3	0.0
1997	B	3	0.58	0.16	--	--
1997	B	3	0.89	0.16	--	--
1997	B	3	1.19	0.17	--	--
1997	B	3	1.45	0.19	--	--
1997	B	3	1.68	0.17	--	--
1997	B	3	2.03	0.16	--	--
1997	B	3	2.29	0.16	--	--
1997	B	4	0.13	0.16	41.0	0.0
1997	B	4	0.36	0.21	62.0	6.5
1997	B	4	0.61	0.19	133.3	4.3
1997	B	4	0.84	0.18	198.9	0.0
1997	B	4	1.22	0.16	281.1	5.0
1997	B	4	1.50	0.14	105.0	8.2
1997	B	4	1.85	0.14	113.7	13.7
1997	B	4	2.13	0.16	135.0	19.9
1997	C	1	0.08	0.15	73.9	23.1
1997	C	1	0.33	0.25	75.5	11.8

Year	Group	Repetition	Depth (m)	θ	Cl^{-1} (mg/L)	NO$_3$-N(mg/L)
1997	C	1	0.56	0.23	167.9	4.2
1997	C	1	0.81	0.16	189.8	--
1997	C	1	1.02	0.16	1330.9	5.8
1997	C	1	1.19	0.18	678.9	6.9
1997	C	1	1.32	0.18	957.5	10.8
1997	C	1	1.57	0.18	722.5	15.6
1997	C	1	1.83	0.16	1389.4	33.2
1997	C	1	2.24	0.16	1612.5	46.7
1997	C	1	2.41	0.15	1113.1	34.6
1997	C	2	0.10	0.14	56.8	0.0
1997	C	2	0.38	0.23	54.2	9.5
1997	C	2	0.53	0.21	149.9	9.9
1997	C	2	0.81	0.20	178.0	6.1
1997	C	2	1.04	0.22	212.1	4.0
1997	C	2	1.27	0.20	317.8	0.0
1997	C	2	1.47	0.19	229.6	4.3
1997	C	2	1.70	0.20	265.2	7.0
1997	C	2	1.91	0.20	365.5	10.3
1997	C	2	2.03	0.16	392.9	11.9
1997	C	2	2.29	0.17	441.1	14.6
1997	C	2	2.51	0.16	555.6	16.6
1997	C	3	0.05	0.16	14.1	7.1
1997	C	3	0.28	0.20	24.8	5.6
1997	C	3	0.53	0.18	31.4	4.0
1997	C	3	0.76	0.17	59.9	8.8
1997	C	3	0.97	0.16	86.0	5.8
1997	C	3	1.24	0.20	86.4	0.0
1997	C	3	1.60	0.16	94.3	8.2
1997	C	3	1.80	0.21	56.0	7.3
1997	C	3	1.98	0.14	66.5	10.3
1997	C	3	2.18	0.15	56.4	12.2
1997	C	4	0.08	0.16	--	--
1997	C	4	0.33	0.24	61.2	0.0
1997	C	4	0.58	0.20	78.9	4.5
1997	C	4	0.94	0.16	230.8	5.0
1997	C	4	1.24	0.16	246.4	0.0
1997	C	4	1.50	0.16	318.9	5.1
1997	C	4	1.78	0.16	222.9	8.9
1997	C	4	1.98	0.16	258.0	13.0
1997	C	4	2.29	0.18	335.3	6.5
1997	D	1	0.10	0.18	24.9	27.0
1997	D	1	0.36	0.25	32.9	28.3
1997	D	1	0.61	0.22	--	--
1997	D	1	0.84	0.21	59.9	30.7

Year	Group	Repetition	Depth (m)	θ	Cl^{-1} (mg/L)	NO_3-N(mg/L)
1997	D	1	1.07	0.20	65.3	17.7
1997	D	1	1.27	0.20	28.1	14.7
1997	D	1	1.60	0.15	149.0	31.5
1997	D	1	1.80	0.15	143.5	41.8
1997	D	1	1.98	0.15	117.8	50.1
1997	D	1	2.21	0.15	170.0	70.4
1997	D	2	0.08	0.13	24.7	83.0
1997	D	2	0.30	0.24	42.8	27.6
1997	D	2	0.56	0.19	27.7	18.4
1997	D	2	0.81	0.18	46.2	25.2
1997	D	2	1.07	0.18	46.3	40.8
1997	D	2	1.30	0.16	45.2	35.6
1997	D	2	1.47	0.16	40.2	31.6
1997	D	2	1.68	0.16	105.6	73.0
1997	D	2	1.91	0.15	88.2	55.2
1997	D	2	2.26	0.18	57.3	35.1
1997	D	3	0.08	0.15	45.8	20.5
1997	D	3	0.30	0.26	29.8	17.5
1997	D	3	0.56	0.21	--	--
1997	D	3	0.79	0.19	61.1	22.9
1997	D	3	1.09	0.17	147.7	27.7
1997	D	3	1.37	0.19	165.2	49.0
1997	D	3	1.60	0.15	208.8	76.6
1997	D	3	1.93	0.15	--	--
1997	D	3	2.21	0.15	--	--
1997	D	4	0.05	0.14	34.9	6.1
1997	D	4	0.28	0.22	49.1	10.8
1997	D	4	0.48	0.24	54.1	21.7
1997	D	4	0.74	0.20	--	--
1997	D	4	1.19	0.17	157.3	14.4
1997	D	4	1.45	0.16	161.2	30.0
1997	D	4	1.68	0.17	147.1	45.6
1997	D	4	2.01	0.15	109.9	47.5
1997	D	4	2.21	0.15	115.9	54.8
1998	A	1	0.08	0.09	32.6	8.3
1998	A	1	0.33	0.20	48.2	0.6
1998	A	1	0.58	0.21	129.6	0.4
1998	A	1	0.84	0.18	249.0	0.3
1998	A	1	1.09	0.20	278.6	0.0
1998	A	1	1.27	0.19	243.4	0.4
1998	A	1	1.52	0.16	210.5	1.7
1998	A	1	1.78	0.16	201.8	2.8
1998	A	1	2.11	0.16	140.2	0.0
1998	A	2	0.18	0.16	52.4	0.4

Year	Group	Repetition	Depth (m)	θ	Cl^{-1} (mg/L)	NO_3-N(mg/L)
1998	A	2	0.43	0.15	145.4	0.0
1998	A	2	0.69	0.14	310.6	0.0
1998	A	2	0.94	0.16	247.3	0.0
1998	A	2	1.17	0.18	207.5	0.0
1998	A	2	1.40	0.16	132.5	0.0
1998	A	2	1.60	0.16	130.9	0.0
1998	A	2	1.85	0.15	109.9	0.0
1998	A	2	2.13	0.16	97.1	0.0
1998	A	2	2.36	0.16	95.4	0.0
1998	A	2	2.59	0.16	127.7	0.0
1998	A	2	2.82	0.19	127.7	3.2
1998	A	2	3.05	0.16	130.8	7.3
1998	A	2	3.30	0.15	147.8	11.0
1998	A	3	0.15	0.21	60.7	3.9
1998	A	3	0.41	0.19	--	--
1998	A	3	0.66	0.15	212.6	0.0
1998	A	3	0.91	0.17	207.5	0.4
1998	A	3	1.17	0.20	174.1	0.0
1998	A	3	1.37	0.18	177.3	0.0
1998	A	3	1.63	0.14	107.3	1.2
1998	A	3	1.88	0.14	244.2	18.0
1998	A	3	2.13	0.15	226.3	31.8
1998	A	3	2.34	0.15	254.3	50.1
1998	A	4	0.15	0.16	53.9	1.9
1998	A	4	0.38	0.15	112.0	0.7
1998	A	4	0.64	0.16	212.1	0.4
1998	A	4	0.89	0.18	231.2	0.0
1998	A	4	1.12	0.16	147.6	0.0
1998	A	4	1.40	0.15	124.3	0.0
1998	A	4	1.68	0.17	78.0	0.0
1998	A	4	1.91	0.16	98.9	0.0
1998	A	4	2.18	0.17	89.5	2.3
1998	A	4	2.39	0.19	--	--
1998	A	4	2.67	0.17	--	--
1998	A	4	2.92	0.16	166.6	23.3
1998	A	4	3.15	0.15	147.2	29.7
1998	A	4	3.38	0.15	112.9	23.7
1998	B	1	0.10	0.16	19.8	12.2
1998	B	1	0.36	0.22	24.0	1.8
1998	B	1	0.61	0.17	47.8	0.6
1998	B	1	0.94	0.19	87.8	0.0
1998	B	1	1.14	0.19	128.1	0.0
1998	B	1	1.40	0.17	98.6	0.0
1998	B	1	1.60	0.16	120.8	1.0

Year	Group	Repetition	Depth (m)	θ	Cl^{-1} (mg/L)	NO$_3$-N(mg/L)
1998	B	1	1.85	0.16	112.1	1.8
1998	B	1	2.11	0.16	91.7	4.7
1998	B	1	2.41	0.17	76.1	2.7
1998	B	1	2.67	0.18	87.4	6.2
1998	B	1	2.92	0.17	97.1	8.9
1998	B	1	3.18	0.17	88.2	11.1
1998	B	2	0.08	0.22	20.5	0.0
1998	B	2	0.33	0.23	25.9	0.8
1998	B	2	0.58	0.22	66.2	0.0
1998	B	2	0.84	0.21	133.8	0.0
1998	B	2	1.12	0.21	197.8	0.0
1998	B	2	1.45	0.17	165.3	0.0
1998	B	3	0.15	0.16	22.8	0.0
1998	B	3	0.41	0.19	84.2	1.1
1998	B	3	0.66	0.18	209.9	0.6
1998	B	3	0.91	0.17	223.4	0.0
1998	B	3	1.17	0.18	194.6	1.0
1998	B	3	1.42	0.18	206.4	3.9
1998	B	3	1.68	0.15	271.2	7.4
1998	B	3	1.93	0.15	300.5	9.4
1998	B	3	2.16	0.15	413.8	6.1
1998	B	3	2.41	0.15	382.1	18.4
1998	B	3	2.67	0.15	357.9	18.6
1998	B	3	2.90	0.15	367.6	18.9
1998	B	3	3.20	0.17	598.2	25.3
1998	B	4	0.13	0.12	63.6	2.2
1998	B	4	0.38	0.14	154.2	2.9
1998	B	4	0.64	0.14	200.0	0.7
1998	B	4	0.89	0.14	178.7	0.4
1998	B	4	1.14	0.14	84.2	0.3
1998	B	4	1.42	0.15	--	--
1998	B	4	1.68	0.19	--	--
1998	B	4	2.01	0.16	120.1	16.9
1998	C	1	0.10	0.17	--	--
1998	C	1	0.36	0.16	53.0	5.1
1998	C	1	0.64	0.17	58.4	1.9
1998	C	1	0.91	0.18	157.6	1.3
1998	C	1	1.19	0.20	359.9	3.3
1998	C	1	1.52	0.17	457.5	8.1
1998	C	1	1.78	0.16	--	--
1998	C	1	2.03	0.15	484.3	15.1
1998	C	1	2.26	0.16	637.2	19.4
1998	C	1	2.54	0.16	567.2	18.5
1998	C	1	2.77	0.16	412.9	11.0

Year	Group	Repetition	Depth (m)	θ	Cl^{-1} (mg/L)	NO_3-N(mg/L)
1998	C	1	3.02	0.16	675.9	28.2
1998	C	1	3.20	0.16	593.5	24.3
1998	C	1	3.40	0.16	588.4	23.4
1998	C	2	0.08	0.12	47.2	2.6
1998	C	2	0.33	0.18	56.1	0.0
1998	C	2	0.58	0.17	55.2	0.0
1998	C	2	0.84	0.17	114.2	0.0
1998	C	2	1.17	0.20	160.1	0.0
1998	C	2	1.40	0.20	154.3	0.0
1998	C	2	1.65	0.19	184.5	1.1
1998	C	2	1.91	0.18	212.0	3.5
1998	C	2	2.16	0.18	279.6	6.2
1998	C	2	2.41	0.15	448.5	8.3
1998	C	2	2.69	0.16	406.3	6.7
1998	C	2	2.90	0.16	416.4	3.0
1998	C	2	3.10	0.16	520.3	4.3
1998	C	3	0.15	0.16	34.7	8.3
1998	C	3	0.43	0.22	32.5	0.5
1998	C	3	0.69	0.17	83.6	0.5
1998	C	3	0.91	0.17	91.3	0.4
1998	C	3	1.17	0.19	87.6	0.0
1998	C	3	1.45	0.18	76.2	0.0
1998	C	3	1.70	0.17	72.4	2.5
1998	C	3	1.96	0.17	58.9	7.0
1998	C	4	0.08	0.13	34.5	1.2
1998	C	4	0.33	0.17	115.0	0.5
1998	C	4	0.58	0.15	--	--
1998	C	4	0.84	0.17	199.2	0.0
1998	C	4	1.14	0.16	201.9	0.0
1998	C	4	1.40	0.17	--	--
1998	C	4	1.65	0.17	102.7	2.8
1998	C	4	1.93	0.15	93.5	7.0
1998	C	4	2.13	0.15	102.1	6.3
1998	D	1	0.05	0.17	33.6	5.0
1998	D	1	0.25	0.22	37.6	--
1998	D	1	0.51	0.17	--	--
1998	D	1	0.76	0.19	26.6	9.9
1998	D	1	1.02	0.19	31.3	4.6
1998	D	1	1.17	0.21	27.6	14.5
1998	D	1	1.42	0.18	49.0	20.5
1998	D	2	0.13	0.16	--	--
1998	D	2	0.41	0.17	8.9	2.2
1998	D	2	0.69	0.18	19.4	0.8
1998	D	2	0.97	0.16	34.4	1.4

Year	Group	Repetition	Depth (m)	θ	Cl^{-1} (mg/L)	NO$_3$-N(mg/L)
1998	D	2	1.22	0.18	51.3	4.1
1998	D	2	1.50	0.14	68.4	21.0
1998	D	2	1.68	0.17	57.5	25.7
1998	D	3	0.18	0.22	21.3	0.0
1998	D	3	0.43	0.19	27.1	0.0
1998	D	3	0.69	0.16	44.1	1.5
1998	D	3	0.91	0.19	79.7	8.3
1998	D	3	1.07	0.21	144.5	8.8
1998	D	3	1.32	0.15	299.2	16.2
1998	D	3	1.57	0.15	339.3	19.7
1998	D	3	1.80	0.15	180.7	7.8
1998	D	3	2.06	0.18	249.0	7.7
1998	D	3	2.36	0.21	106.6	5.1
1998	D	3	2.54	0.15	443.1	16.7
1998	D	3	2.79	0.15	808.5	27.2
1998	D	3	3.05	0.14	595.6	18.5
1998	D	3	3.20	0.16	510.5	17.4
1998	D	3	3.43	0.15	781.6	25.3
1998	D	4	0.08	0.15	60.2	23.0
1998	D	4	0.33	0.15	4.7	2.1
1998	D	4	0.64	0.13	--	--
1998	D	4	0.97	0.15	49.7	4.5
1998	D	4	1.24	0.17	64.3	8.2
1998	D	4	1.42	0.15	76.8	17.6
1998	D	4	1.68	0.18	--	--
1998	D	4	1.93	0.18	54.3	26.2
1998	D	4	2.18	0.16	54.1	27.5
1998	D	4	2.44	0.17	75.8	32.1
1998	D	4	2.59	0.17	80.8	28.2

VITA

John S. Tyner

Candidate for the Degree of

Doctor of Philosophy

Thesis: ESTIMATING FLOW AND TRANSPORT PARAMETERS OF
UNSATURATED POROUS MEDIA

Major Field: Biosystems Engineering

Biographical:

Education: Graduated from Putnam City High School, Oklahoma City, Oklahoma
in 1986; received a Bachelor of Science in Geology from University of
Oklahoma, Norman, Oklahoma in 1990; received a Master of Science
degree in Geology (hydrology option) from San Diego State University,
San Diego, California in 1998; completed the requirements for the Doctor
of Philosophy degree in Biosystems Engineering at Oklahoma State
University, Stillwater, Oklahoma in August, 2001.

Experience: Served as a United States Naval Officer aboard the USS COPLAND
(FFG-25) with homeport of San Diego, California, 1991-1993; employed
by Aqui-Ver Inc. in San Diego, California as a hydrologist, 1995-1996;
employed by McLaren/Hart Inc. in Irvine California as an Assistant
Geoscientist, 1996-1997; employed by the University of Phoenix in
Oklahoma City, Oklahoma as Adjunct Faculty, 2000-2001; employed by
the Biosystems and Agricultural Engineering Department at Oklahoma
State University in Stillwater, Oklahoma as a Research/Teaching Assistant,
1998 to present.

Awards and Professional Affiliations: 2001 Phoenix Award of Excellence, Sigma
Xi (International Honor Society for Scientific and Engineering Research),
Alpha Epsilon (Agricultural Engineering Honor Society), Gamma Sigma
Delta (Agriculture Honor Society), American Geophysical Union,
American Society of Agricultural Engineers.